THESIS

LASER DAMAGE THRESHOLDS OF EX-VIVO PIG AND RABBIT CORNEAS AT 2.5 AND 2.7 μm WITH 8 NANOSECOND LASER PULSE DURATION

Submitted by

Yuanqing Guo

Department of Environmental and Radiological Health Sciences

In partial fulfillment of the requirements

For the Degree of Master of Science

Colorado State University

Fort Collins, Colorado

Summer 2011

Master's Committee:

Advisor: Thomas Johnson

Alexander Brandl
Elliot R. Bernstein

ABSTRACT

LASER DAMAGE THRESHOLDS OF EX-VIVO PIG AND RABBIT CORNEAS AT 2.5 AND 2.7 μm WITH 8 NANOSECOND LASER PULSE DURATION

With the rapid development of advanced laser technology, lasers have been widely applied to research, industry, medicine, military, and consumer products, particularly in the infrared (IR) spectral region. Consequently, safety has been a major concern not only for people who develop and operate lasers, but also for people who use products integrated with lasers. To establish specific laser safety standards for eye protection, many laser safety studies have been conducted for determination of the retina damage threshold in the visible spectral region. The damage threshold for the cornea, a major damage target in the IR wavelength range, however, has not been well established, especially for short laser pulse durations (ns). The purpose of this work was to determine the damage thresholds of the cornea at 2.5 and 2.7 μm with 8 ns laser pulses using ex-vivo pig and rabbit eye models. In addition, due to the difference of water absorption coefficients at these two wavelengths (the water absorption coefficient at 2.7 μm is about 4-5 times of that at 2.5 μm), the role of water absorption for corneal damage was estimated through comparison of damage thresholds at these two wavelengths. Based on our experimental results, both pig and rabbit eyes have similar damage thresholds (ED_{50}) of 0.81 J/cm^2 at 2.7 μm and 3.66 J/cm^2 at 2.5 μm. The ratio between the damage

thresholds at these two wavelengths is 4.5, which is in good agreement with the ratio of the water absorption coefficients at these two wavelengths. This finding suggests that water absorption in the IR spectral region plays an important role in the damage threshold of the cornea. In addition, temperature changes on the cornea induced by laser energy absorption at varied radiant exposure were monitored through an infrared camera (ThermaCAM^{TM} S65). Results indicate that the increase of temperature on the corneal surface is proportional to the radiant exposure, and with a measured damage threshold of 0.7 ^{o}C above ambient.

ACKNOWLEDGMENTS

This work was carried out and completed under the guidance of my Master degree advisor, Dr. Thomas E. Johnson. His deep and broad knowledge in Health Physics, insights, patience, understanding and all around support have been invaluable. I would like to thank him for his great contributions and support toward this thesis.

The experimental work of this thesis was carried out in Dr. Elliot R. Bernstein's lab in the Chemistry Department. I would like to express my thanks to him for his kindness to let me use his facilities, and also for his constructive discussion and suggestions during the completion of this work. I also would like to thank Dr. Alexander Brandl, one of my committee members, for his comments and effort in improving this thesis.

I would like to thank Ed Kelly for all of his excellent help in the setup and operation of the infrared camera as well as his very valuable discussion about my experiments. I also would like to express my thanks to Dr. Joong-Won Shin for his kind assistance in the operation of the OPO IR laser systems. Dennis Madden, the lab coordinator at the Veterinary Teaching Hospital at CSU provided me ex-vivo pig eyes. I would like to thank him for his assistance and friendliness. Many thanks to all of my Health Physics classmates for their useful discussions and great cooperation in team course work. I also would like to thank Ms. Julie Asmus, Ms. Jeanne Brockway and Ms. Aimee Oke for their kind assistance during the course of my study.

Finally, I would like to thank my wife, Liping Yi, my daughter, Quiana Ziqi Guo, and my son, Jack Zile Guo for their love and support during this busy and fruitful study period.

TABLE OF CONTENTS

CHAPTER 1: INTRODUCTION

1.1 Introduction

Due to laser's unique characteristics, such as monochromaticity, high intensity, and coherence, it has been widely applied in all different kinds of fields since its development in 1960's [1]. Many of these fields include industry, medicine, military, scientific research, and consumer products. For example, high power lasers have been used in material and semiconductor industries for precise cutting, drilling, and ablation of all kinds of materials [2, 3]. Similar to the industry applications, high power lasers have also been used for surgical cutting and ablation in medical treatment [4], and nowadays many high performance lasers are used for treatment of diseases on delicate and complex organs including eye, heart, and other organs [5]. In scientific research, lasers have been widely used as light source for optical studies [6], molecular spectroscopy [7], and molecular biology [8] as well. Moreover, with the rapid development of new laser techniques, the application of lasers in consumer products, such as laser printers and scanners, optical storage and reading devices, laser pointers, and infrared (IR) laser monitors, has increased tremendously in the past decades.

With the rapid expansion of laser application in all these fields, the laser radiation exposure hazard and laser safety have been a major concern not only for people who develop and operate lasers, but also for people who use products integrated with lasers. This directly triggered an urgent requirement for scientifically based laser safety standards.

The laser, defined as light amplification by stimulated emission of radiation, is classified as non-ionizing radiation as compared to other high energy ionizing radiations, such as X-ray and gamma ray. The first safety limits for exposure to laser radiation in the United States were formulated during 1962-1963 for use in the military services [9]. Since then, many laser exposure limits and safety standards have been developed in the US and Great Britain; however, the first widespread public exposure limits of the American Conference of Government Industrial Hygienists (ACGIH) were not given until 1968 [10]. One year later, at the request of the U.S. Department of Labor, the American National Standards Institute (ANSI) started to develop a consensus standard for the “safe use of laser and masers”, which was redefined as “Safe Use of Lasers” and designated as Standards Committee Z-136 [11]. This standard has been revised many times, and now forms the basis of Federal regulations concerning laser safety and standard for several organizations, such as the Center for Devices and Radiological Health (CDRH) of the Food and Drug Administration (FDA), and the Department of Labor's Occupational Safety and Health Administration (OSHA). The CDRH regulations involving laser product and its classification can be found in 21 CFR 1040.10. OSHA, however, does not have a comprehensive laser standard and some of its regulations relevant to the construction industries can be found in 29 CFR 1926.54 [12]. In addition, several state governments and the Council of Radiation Control Program Directors (CRCPD) have developed a model state standard for laser safety.

Laser exposure limits and laser safety standards were developed based on the biological effects of laser beam exposure. Laser-tissue interaction mechanisms vary with tissue characteristics and laser parameters. There are five main categories of laser-tissue

interaction types including photochemical interactions, thermal interactions, photo ablation, plasma-induced ablation, and photodisruption depending on the laser spectral region and power density [13]. The two major concerns of the laser exposure hazard to the human body, thermal injury to the skin and eye injury, involve thermal interaction and photo ablation as the main interaction mechanisms. The basic principle for thermal injury is exceeding a certain temperature on the exposed tissue by absorbing photon energy from a laser beam with long pulse duration and low power density (typical 10 - 10^6 W/cm^2) resulting in damage through coagulation, vaporization, cabonization, or melting. When a relatively higher laser power density (typical power density of 10^7-10^8 W/cm^2) is applied to human tissue, photo ablation becomes the primary interaction mechanism, in which the damage is induced by excitation then dissociation.

Unlike ionizing radiation, a threshold of laser radiation injury to the skin and eye exists, whether thermal interaction or the photo ablation interaction mechanism occurs. Therefore, determination of damage threshold for laser radiation exposure to skin and eye provides the most important biologic effect data for the establishment of laser exposure limits for laser safety standards.

As one of the most critical hazards from laser radiation exposure, the eye represents a potential for injury to several different structures, which generally depends on which structure absorbs the most radiation energy. The absorption of the laser radiation by the two most sensitive structures of an eye, the retina and cornea, varies greatly with laser wavelength. This results in a strong wavelength dependence of the laser injury to the retina and cornea. For instance, in the visible and near IR spectral region (0.4 - 1.4 μm), laser injuries occur mostly on the retina due to the high transmission of

visible light through the cornea and the high radiant energy absorbed per volume of tissue in retina [14, 15]. On the other hand, injuries occur primarily on the cornea due to its strong absorption in the ultra-violet (UV), middle and far IR spectral regions [9, 16]. Laser safety standards for eye protection have been well established in the visible and near IR spectral region, but not in middle IR region, particularly for short laser pulses. Therefore, to provide the necessary biological effects data for input to laser safety standards, measurements and determination of the laser damage thresholds of the cornea at middle IR wavelengths (2.5 and 2.7 μm) with short pulse duration were conducted using ex-vivo rabbit and pig cornea models.

1.2 Structures of eye and cornea

To help better understand the laser injury to the eye, especially the cornea, a brief review of the anatomy of an eye is given in this section. The primary structures of an eye comprise a cornea, an iris for pupil size control, a lens for light focusing, and multi layers of the retina. Light passes through the cornea, the iris and the lens, and is magnified onto the retina where the light signal is sensed and converted into neural impulse signals that lead to vision by two types of photoreceptor cells: rods and cones. The ocular focus region is around a wavelength rage of 0.4-1.4 μm. Therefore, when visible or near IR laser beams are employed, the light is mostly focused on the retina, and may damage the retinal tissue if the radiation exposure exceeds the damage threshold.

The cornea of an eye is the clear, dome-shaped outmost layer that is exposed directly to the environment. Due to the lack of blood vessels in the corneal tissue, the only way for the cornea to receive its nourishment is from tears and the aqueous humor that fills the chamber behind it. The corneal structure is organized in five basic layers

(See Figure 2 in Ref. [17]), which are the epithelium, Bowman's layer, Stroma, Descemets' membrane and endothelium. The Epithelium is the outmost region of the cornea. It comprises about 10 percent of the corneal tissue thickness, and provides protection to the eye from invasion of foreign materials, such as dust, water and bacteria. The transparent Bowman's layer, which appears only in the cornea of the primates, lies directly below the basement membrane of the epithelium. Stroma is the layer beneath the Bowman's layer, which comprises about 90 percent of the corneal tissue's thickness. The corneal layer of an eye has strong absorption in the UV (< 0.4 μm), and the middle and far IR spectral region (1.4 -1000 μm). Thus, if an eye is exposed to a laser radiation within these wavelengths, the damage will be on the corneal layers if the exposure exceeds the damage threshold. In addition, water absorption of IR laser light might play an important role in causing damage to the cornea because most of the content of the corneal layer is water [17, 18].

1.3 Basic concepts and definitions related to this work

A few important concepts and definitions that related to this work are introduced in this section for quick reference. Most of these concepts have been well defined in the ANIS Z136.4 standard, and are directly cited here [19].

A laser beam is characterized by monochromaticity, high intensity and coherence. The most important parameters of a laser that relate to the measurement of the damage threshold of a tissue are wavelength (or Frequency), energy or power, pulse duration, and beam size. Laser wavelength is defined as the distance between two successive points on a periodic electromagnetic wave which have the same phase. It covers a broad electromagnetic spectral range of UV (<0.4 μm), visible (0.4 - 0.7 μm), near IR (0.7 - 1.4

μm), and mid and far IR (1.4 - 1000 μm). The relationship between the laser wavelength and frequency is expressed by equation (1),

$$\lambda = c / \nu \quad (1)$$

where λ, c and ν are the wavelength, the speed of light, and the frequency, respectively. The wavelengths (2.5 and 2.7 μm) used in this work are in the mid-IR spectral range.

Laser pulse duration is the duration during which the radiation is emitted. It is usually measured as the time interval between the half energy of power points on the leading and trailing edges of the pulse. If the laser pulse duration is longer than 0.25 s, the laser is usually said to be operated in a continuous wave (CW) mode rather than in a pulse mode. In this work, the laser is run in a pulse mode with a pulse duration of 8 ns.

Energy is used to characterize the output from a pulsed laser, and is generally expressed in Joules (J). Power is the rate of the laser energy emission, and is expressed in Watts (W), or Joule per second (J/s).

The beam diameter is defined as the distance between diametrically opposed points in the cross-section of a beam where the power per unit area is 1/e times that of the maximum power per unit area. The size or area of a laser beam can be calculated based on the diameter and the shape of the beam.

With the knowledge of laser energy (or power) and the beam size, the radiant exposure (or irradiance), which is defined as the radiant energy (or power) incident per unit area upon a surface can be calculated. Radiant exposure (or irradiance) is expressed in J/cm^2 (or W/ cm^2).

Besides the above concepts that characterize a laser, several definitions involved in laser safety and standard are defined as following. Effective dose 50 (ED_{50}) is the

exposure that represents 50% probability of injury. It is also frequently referred to as a "threshold" [20]. Maximum permissible exposure (MPE) is defined as the level of laser radiation to which a person may be exposed without hazardous effect or adverse biological changes in the eye or skin. It is expressed in J/cm^2 or W/ cm^2. It is usually set a factor of ten below the ED_{50}.

1.4 Previous studies

Due to the availability of lasers and the susceptibility of the retina to damage by radiation at the visible and near IR spectral region (0.4 – 1.4 μm), most laser safety studies have been conducted to investigate the damage to the retina [21-23]. The injury mechanisms of the retina vary depending upon the wavelength, as well as the exposure duration at the damage threshold. At shorter wavelengths (0.4 - 0.5 μm) of visible radiation, photochemical interaction has been alleged to be the major injury mechanism from lengthy exposure to low intensity laser radiation [24, 25]. However, thermal injury becomes the major interaction mechanism when exposure duration becomes less than a few seconds. Photodisruption might also occur if the exposure duration reaches the nano- or pico- second range.

In the middle IR wavelength range, the ocular media are opaque because of strong absorption of the radiation by the water content in the cornea. Thus thermal damage to the cornea is the primary biologic effect when the eye is exposed to laser radiation in this spectral region. Middle IR radiation exposure to the eye has been studied mostly at 10.6 μm generated from CO_2 lasers [26-28]. Studies indicated that the epithelium and the stroma layers of the corneal tissue were the major damage components at 10.6 μm. Some other studies in the wavelength range of 1.3 - 2.1 μm have been conducted for

investigation of endothelial damage [29, 30]. In these studies, endothelial temperature increases close to those in the epithelium and stoma were observed as these wavelengths penetrate the entire cornea thickness and therefore produce more uniform heating.

In the 2.5-4 μm wavelength range, where water displays a broad and varied absorption, a few studies have been conducted to investigate the laser damage thresholds of the cornea using ex-vivo animal eye models [18, 31, 32]. Due to the different pulse duration, wavelength, and spot size used in these studies, it is difficult to tell which laser parameter, such as pulse duration, beam size, or wavelength plays the most important role in the determination of the laser damage threshold. For example, Muller and Ham had determined the ED_{50} of the rabbit cornea to be 6.99 J/cm^2 at 2.9 μm with a 100 ns pulse duration and 2.0 cm^2 beam size [31], and Fyffe and co-workers determined the ED_{50} of the pig cornea to be 6.7 J/cm^2 at 3.8 μm with an 8 μs pulse duration and 4.0 cm^2 beam size [18]. Although all three laser parameters are different in these two studies, they obtained very similar ED_{50}s for the cornea for the two types of animals. There is a significant difference in the water absorption coefficient between 2.9 (maximum absorption) and 3.8 μm [33]. Hypothetically, water absorption plays an important role in the damage to the corneal tissue, such that the ED_{50} at 2.9 μm should be smaller than that at 3.8 μm. However, this difference might be masked by the effect of different pulse durations applied in these two studies. In order to understand the roles of different laser parameters in the damage of the cornea, and provide effective biological effect data for the determination of a laser exposure limit in the wavelength range of 2.5 - 4 μm, the damage thresholds of ex-vivo pig and rabbit corneas at 2.5 and 2.7 μm with 8 ns pulses were investigated in this work.

1.5 Objective and Goals of this study

The objective of this study was to investigate the damage thresholds of ex-vivo pig and rabbit corneas at IR wavelengths (2.5 and 2.7 μm), and to examine the relationship between the damage thresholds and the water absorption at different laser wavelengths. As mentioned in the Previous Study section, most of the studies on the laser damage to eyes have been focused on the visible and near IR wavelength region, which give a good understanding of the damage to the retina, and the corresponding laser safety standards have been well established. In the middle IR wavelength range, however, light transmission is significantly reduced due to absorption in the cornea, which results in the laser damage occurring on the cornea rather than the retina. The corresponding laser safety standards for the middle IR wavelength have not been well established, especially for short laser pulse durations. With the rapid development of ultrafast lasers, the safety standards for short pulse laser become more and more important. In addition, comparison of damage thresholds between fresh and frozen eyes, and between pig and rabbit eyes is another objective for this work.

Therefore, the primary goals of this work are to determine the laser damage thresholds of ex-vivo pig and rabbit corneas at two IR wavelengths (2.5 and 2.7μm) with ns pulse duration to provide data that may assist in establishing the laser safety standards in these wavelengths. Based on the similarity or difference of the damage thresholds between different animals (pig and rabbit), we can theorize that the damage thresholds, more importantly the established laser safety standards can be extrapolated to a human being. In addition, by comparing the damage thresholds of the corneas at different wavelengths with different water absorption coefficients, we may develop theories on the

role of water absorption in the damage of the cornea at IR wavelength. Another goal of this study is to measure the temperature change on the cornea at damage thresholds.

CHAPTER 2: EXPERIMENTAL SETUP AND MATERIALS

2.1 Experimental setup

The schematic diagram of the experimental setup used for this study is shown in Figure 2-1. It consists of an optical parametric oscillator (OPO) IR laser system, a magnesium fluoride lens, a pinhole, an eye holder, and a thermal camera. The middle IR laser beam generated by the OPO systems is focused by a magnesium fluoride lens before intercepting the cornea of an eye. The focal length of the lens was 5.2 cm, making it possible to focus the laser beam into a spot size of a few hundred μm in diameter, and to produce a high energy density on the corneal surface.

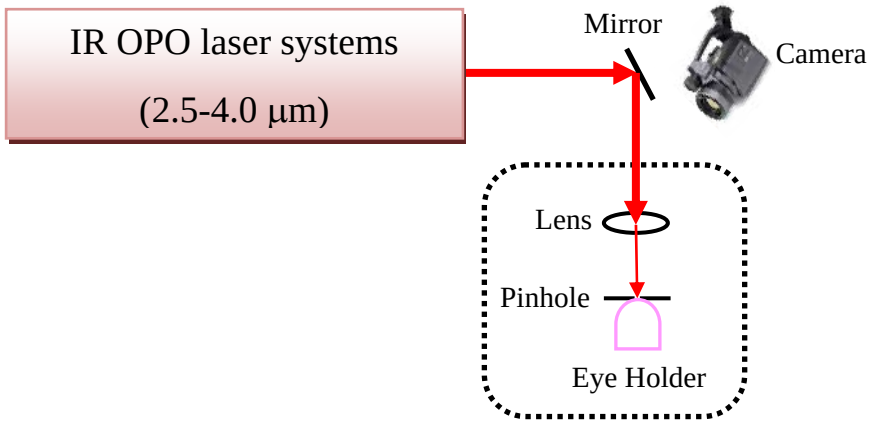

Figure 2-1: The schematic diagram of the experimental setup

The pinhole in front of the eye holder is mounted on a three dimensional translation stage. It is used to determine the size of the beam spot on the cornea, and to predetermine the location of the eye so that the same beam size may be used for each measurement. The eye holder is also mounted on a three dimensional translation stage to locate the eye precisely. The temperature on the cornea's surface was monitored by an IR thermal

camera, one meter away from the eye, and was set in a sharp angle with the incident laser beam. The assembly within the dotted box, including the lens, pinhole and the eye holder is shown in the picture in Figure 2-2.

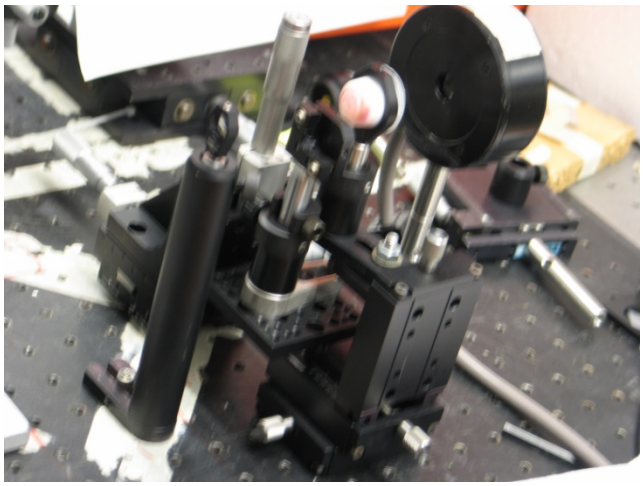

Figure 2-2: Assembly of the lens, pinhole, and the eye holder

2.2 OPO IR Laser systems

The OPO IR laser system was pumped by a neodymium:yttrium aluminum garnet (Nd:YAG) laser (shown in Figure 2-3). The Nd:YAG laser generated a 1064 nm fundamental laser beam with an 8 ns pulse duration. The 1064 nm beam was split into two beams via a beam splitter; one of the beams was doubled to 532 nm through a KDP crystal, and used to pump OPO crystals to produce signal and idler beams. The idler beam was then mixed with the second 1064 nm beam in OPA crystals to produce a wavelength between 2.5 – 5 μm. The laser wavelength was tuned by changing the OPO and OPA crystal angles simultaneously. The repetition frequency of the OPO laser was controlled by the repetition rate of the Nd:YAG laser, which varied from 1 to 10 Hz. All the experimental measurements in this work were performed at a repetition rate of 1 Hz.

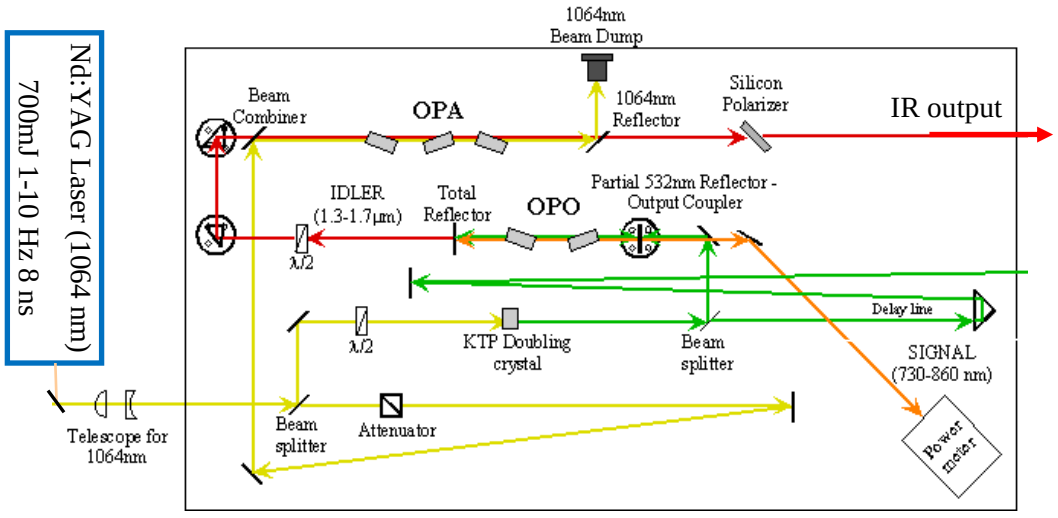

Figure 2-3: Laser Vision OPO/OPA systems producing an IR wavelength of 2.5 - 5.0 μm.

The IR laser pulse profile, detected via a photodiode and recorded by an oscilloscope, is illustrated in Figure 2-4. The black solid circles are experimental measurement points, and the red solid line is the Gaussian fit. The pulse shape shows a Gaussian distribution with a full width at half maximum (FWHM) of 8 ns.

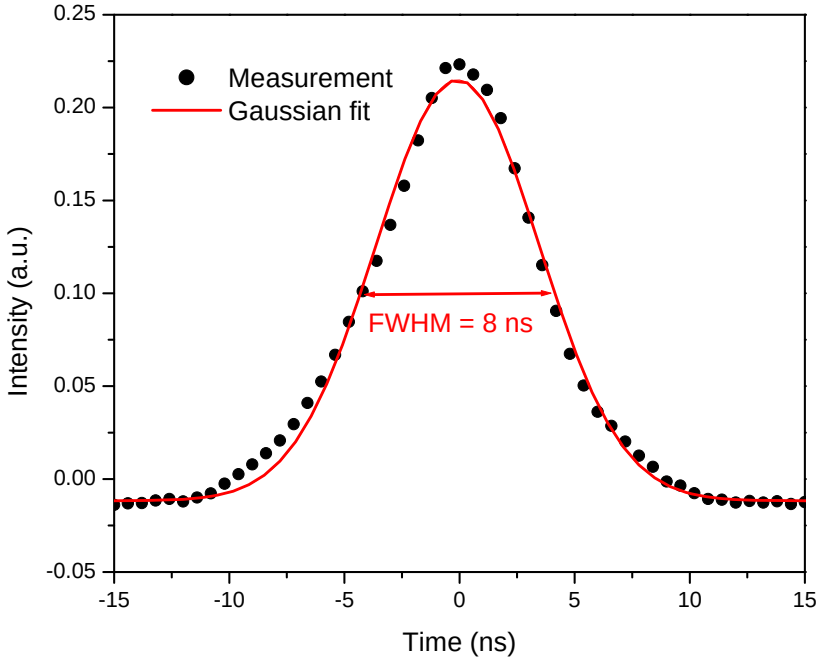

Figure 2-4: The IR Laser pulse profile showing a Gaussian distribution with a FWHM of 8 ns.

2.3 Thermal Camera

The temperature change induced by laser irradiation on the corneal surface was monitored via a thermal camera (Model: TheramCAMS65, FLIR SYSTEMS). The infrared camera measured and imaged the emitted infrared radiation from the corneal surface. Infrared radiation intensity is proportional to the temperature of the region of interest (ROI), making it possible for the camera to show and calculate the temperature change of that region. The camera's detector consists of a 320 × 240 array of micro-bolometer elements, which have responses to infrared radiation in the spectral range from 7.5 to 13 μm. The camera was calibrated by the manufacturer with a sensitivity specification of ± 0.05 ºC with NIST-traceable blackbody sources. The time resolution of the camera was approximately 5 ms.

The thermal camera was mounted on a Davis and Sanford camera tripod (Model: Magnum X3T Tripod). To obtain a good focus of the measured object and catch the most intense radiation from the object, the camera was positioned approximately 1 meter away from the cornea, and aligned at a sharp angle (20-30^{o}) with the incident laser beam. The camera operation and data acquisition were remotely controlled through a computer via a firewire (IEEE 1394) interface. The raw images were stored in the computer, and the temperature for the ROI was extracted using the manufacturer's software, Researcher Pro version 2.8 (FLIR Systems, Wiesbaden, Germany).

2.4 Energy and beam size measurement

The laser energy was measured behind the magnesium fluoride lens via a Nova–P power meter with a PE-10 probe (Ophir-Spiricon), calibrated with a specified uncertainty of 3%. Due to the fluctuation of the output energy from the OPO system, all energies for

the damage threshold calculations were the average values for over 200 pulses with a standard deviation of 10%. The output energy from the OPO system remained constant during each group of measurements, and the radiant exposure was changed via neutral density filters.

The output beam from the OPO system was elliptical. The beam diameters along the major and minor axis were measured using the pinhole aperture method [19]. In this method, as shown in Figure 2-2, a pinhole with a diameter of about 50 μm was set between the focal lens and the power meter. The energy reads from the power meter were recorded as the pinhole was scanned across the two dimensional plane of the laser beam. The beam diameter was defined as the average radial distance between two points where the local beam irradiance drops to 1/e times the center beam irradiance.

2.5 Pig and Rabbit eyes

Pig eyes used in this study were from the Veterinary Teaching Hospital at Colorado State University. Fresh pig eyes were obtained soon after pigs were slaughtered. These eyes were then frozen in a freezer at a temperature of about -10 ^{o}C. Before experimental measurements, the frozen pig eyes were restored back to 14-16 ^{o}C, and rinsed using 0.9% saline solution. In this thesis, the frozen eyes were designated as eyes that had been frozen but restored back to 14-16 ^{o}C before experiments.

The rabbit eyes were obtained from Pel-freez Biological. Both fresh and frozen rabbit eyes have been used for the measurements of the damage threshold of rabbit cornea. Similar to the treatment of pig eyes, frozen rabbit eyes were restored back to 14-16 ^{o}C before experimental measurements, and cleaned and rinsed using 0.9% saline solution. Some sample pig and rabbit eyes with and without laser lesions are presented in

Figure 2-5. Cornea damage was identified by white opacities produced by laser irradiation.

Figure 2-5: Pig (upper left) and rabbit (upper right) eyes without laser lesion; pig eyes with single (bottom left) and multiple laser lesions (bottom right).

CHAPTER 3: MEASUREMENTS AND DATA ANALYSIS

3.1 Beam size measurements

The pinhole method was employed to measure the laser beam diameters at 2.5 and 2.7 μm wavelengths. The measurements for the horizontal and vertical beam directions at 2.5 μm are shown in Figure 3-1. The beam was an elliptical shape rather than circular, and the horizontal direction of the beam exhibited a Gaussian energy distribution. The vertical direction of the beam could still be fitted with a Gaussian distribution, but was not quite as good. Based on the experimental measurements and the theoretical Gaussian fits, the diameters (the average radial distance between two points where the local beam irradiance drops to 1/e times the center beam irradiance) of the major and minor axis of the elliptical beam at 2.5 μm were determined to be 538 ± 30 and 195 ± 4 μm, respectively. For an elliptical beam spot, the area was calculated to be 0.08 mm^2 by the expression $\pi\,(a/2)\,(b/2)$, where a and b were the length of the major and minor axis of the ellipse, respectively.

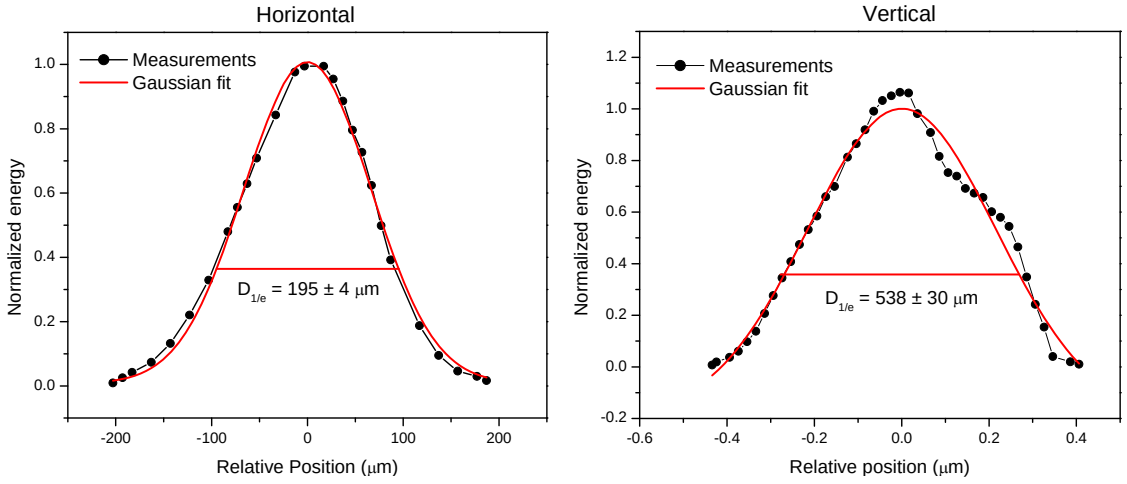

Figure 3-1: Laser beam diameter measurements at the 2.5 μm.

Similar measurements (see Figure 3-2) were also performed at 2.7 μm. The lengths of the major and minor axis of the elliptical beam were determined to be 667 ± 80 and 233 ± 15 μm, which are about 15-20% greater than that at 2.5 μm in both horizontal and vertical directions due to the change of index of refraction at the different wavelengths. The area of the beam spot was calculated to be 0.12 mm^2.

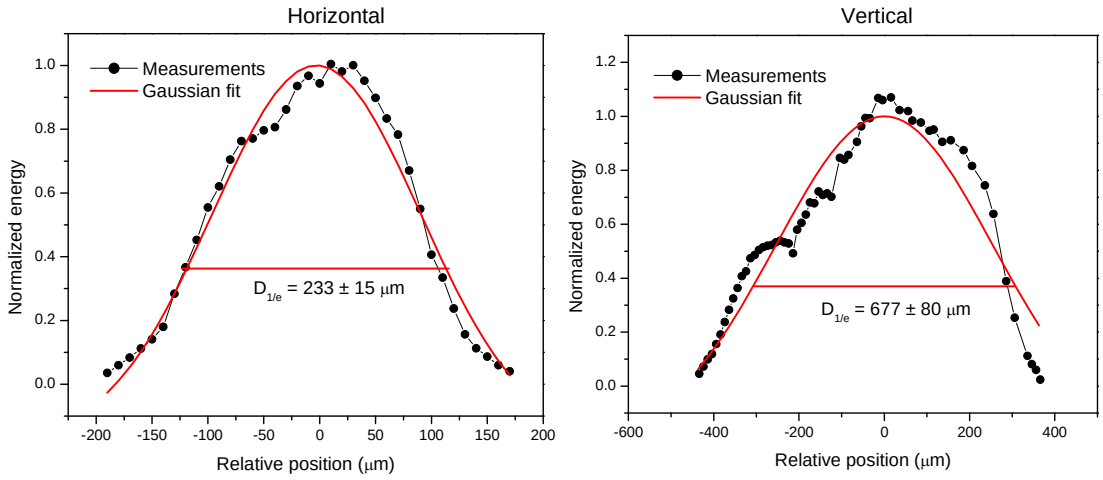

Figure 3-2: Laser beam diameter measurements at the 2.7 μm.

3.2 Temperature monitoring using an IR thermal camera

Temperature monitoring on an object surface using the IR thermal camera was demonstrated by laser irradiation of a post-it paper. The bright spot on the left-hand side screen in Figure 3-3 is the image of the irradiated area of the paper. The temperature scale is displayed on the right-hand side of the screen, which shows how the colors are distributed along various temperatures in the image. For each laser pulse irradiation on the paper, a bright spot was caught on the image. The bright spot then gradually weakened and disappeared over time. The evolution of the temperature on the object surface (post-it paper in this case) was extracted from the recorded images using the

thermal camera's software. For each laser exposure, a rapid increase followed by a slow decay of the temperature on the surface was observed.

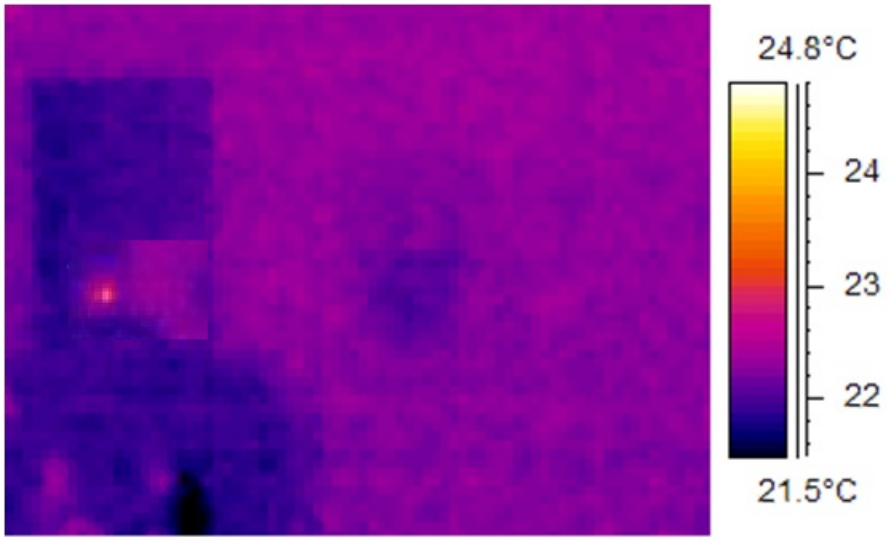

Figure 3-3: A typical image recorded by the IR thermal camera with high temperature exposure spot on the surface of a post-it paper.

The corresponding temperature changes with multi-pulse exposures on the post-it paper were shown in Figure 3-4. Each pulse signal in the plot indicates the temperature evolution initiated by a single radiation exposure. Due to the energy fluctuation among laser pulses, a variation on the temperature change for different exposure pulses was observed in this testing measurement. Nevertheless, partial variation might be caused by the relatively low resolution of the camera.

For laser damage threshold measurements and temperature monitoring on the pig and rabbit corneal surfaces, only single laser exposure was applied for each measurement at a specific laser radiant exposure. By varying the laser radiation exposed on the corneal surface using neutral density filters, the damage thresholds of the pig and rabbit corneas can be determined by identifying the appearance of laser lesions on the corneal surfaces.

As laser energies were varied, the temperature change at each radiant exposure was recorded.

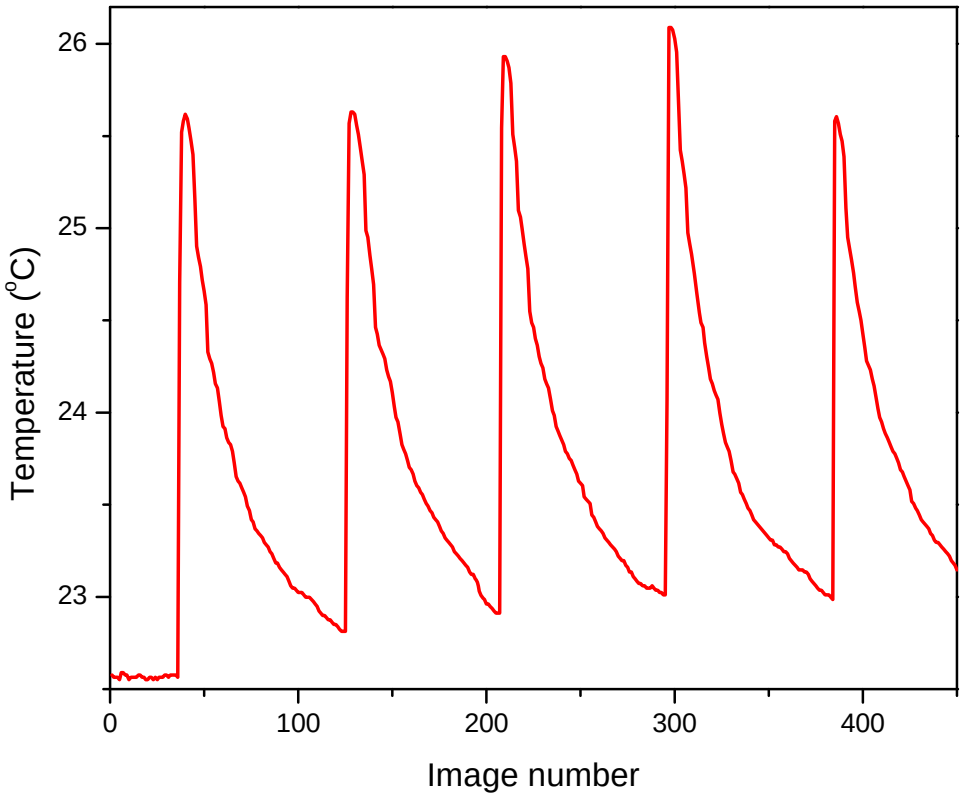

Figure 3-4: Temperature evolution on the surface of a post-it paper with multiple pulse exposures

3.3 Ex-vivo rabbit eye measurements at 2.7 μm

Measurements of both fresh and frozen rabbit eyes were performed at 2.7 μm. Fresh rabbit eyes in an ice bath were received from Pel-freez Biological (Roger, AR) within 24 hours after the rabbits were euthanized. These eyes were left in the lab at room temperature for about 6 hours until their temperatures were 14-16 ^{o}C before experimental measurements were performed. Other rabbit eyes were frozen for 1-7 days before the measurements were carried out. Those frozen eyes were also warmed to 14-16 ^{o}C before experiments. Results of the laser radiation exposure on fresh and frozen rabbit eyes at 2.7 μm are shown in Figures 3-5 and 3-6, respectively. Both fresh and frozen rabbit eyes

presented similar responses to the laser radiation exposures. For each specified radiant exposure, the temperature on the corneal surface first rose rapidly then decayed back to the initial temperature (baseline). Both the temperature changes on the corneal surfaces and the temperature recovery time were proportional to the incident radiant exposures. A maximum temperature change of 2.2 ^{o}C at the available maximum radiation exposure (~ 4.5 J/cm^2) at 2.7 μm was observed, and both fresh and frozen rabbit eyes were damaged at a similar exposure (first observed at 1.29 J/cm^2, 8 ns) with a temperature change of 0.8 - 0.9 ^{o}C.

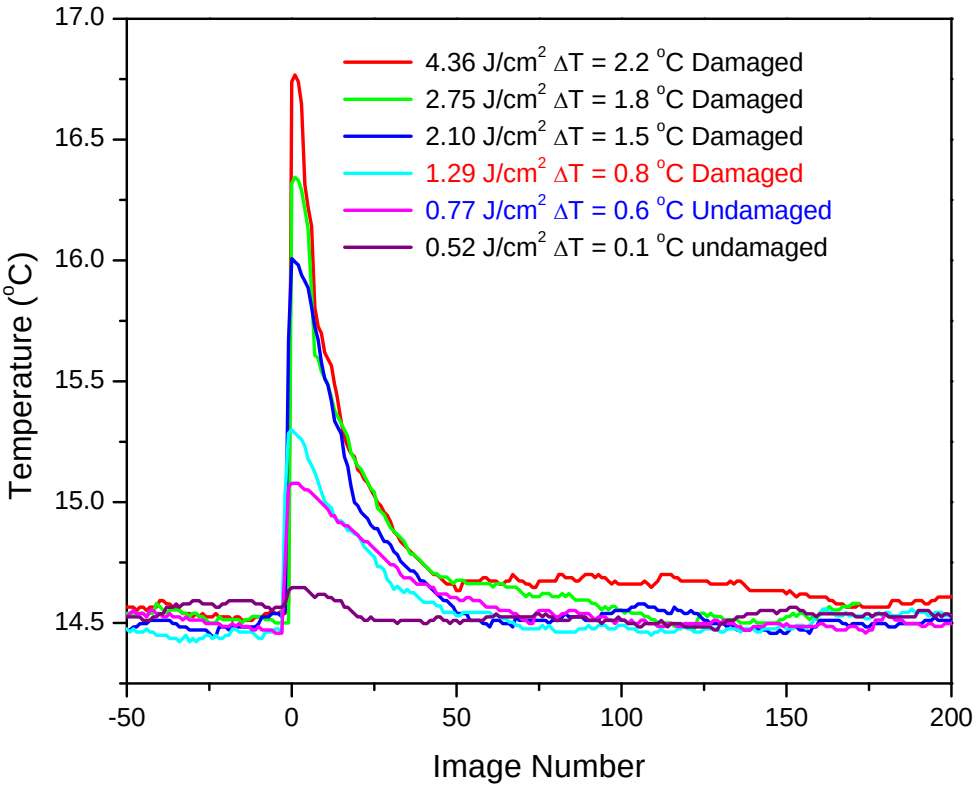

Figure 3-5: Measurements of laser radiation exposure on fresh rabbit corneas at 2.7 μm.

The experimental data for fresh and frozen rabbit eyes are summarized in Tables 3-1 and 3-2, respectively. The “slightly damaged” in the tables is defined as observable light opacity on the cornea. Due to the time consuming and difficulties in alignment of the thermal camera for temperature monitoring on the corneal surface, some more

measurements were performed without a temperature recording. A full list of all measurements with and without temperatures for fresh and frozen rabbit eyes are given in the appendix as tables TA 3-1 and TA3-2. Based on the measurements listed in these two tables, a Probit program was employed to calculate and determine the ED_{50} for the laser irradiation of the rabbit cornea at 2.7 μm [34]. The ED_{50}s for fresh and frozen rabbit corneas at 2.7 μm were determined to be 0.81 and 0.83 J/cm^2, respectively.

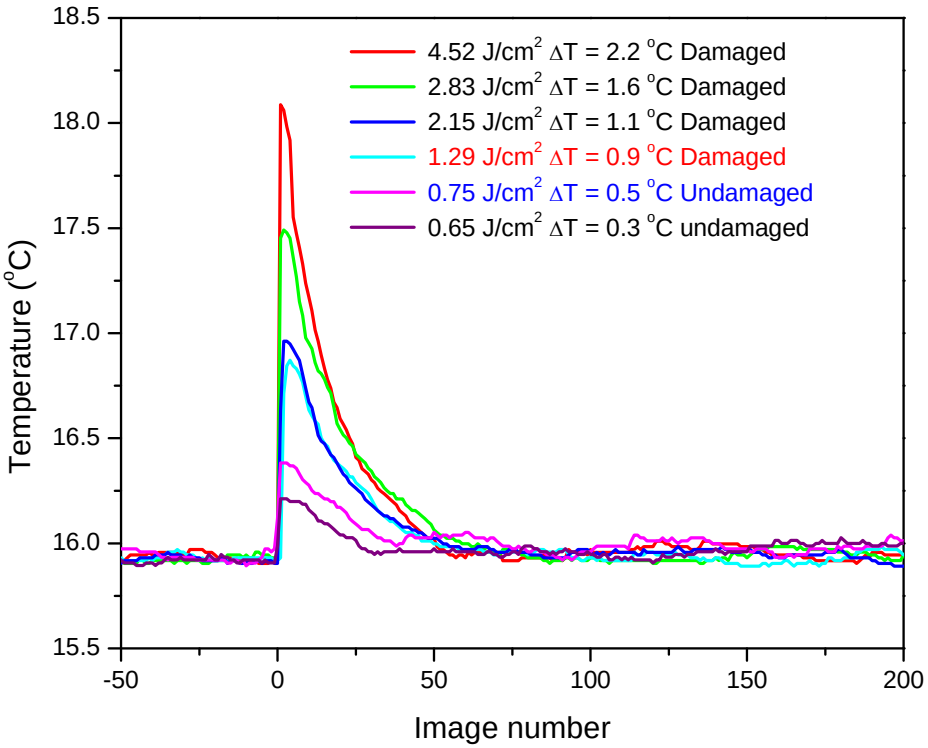

Figure 3-6: Measurements of laser radiation exposure on frozen rabbit corneas at 2.7 μm.

Table 3-1: Measurements of laser exposure on ex-vivo rabbit corneas (Fresh) at 2.7 μm

Radiant exposure (J/cm^2)	Temperature change (^{o}C)	Cornea status
0.52	0.1	Undamaged
0.65	0.4	Undamaged
0.77	0.6	Undamaged
0.91	0.7	Slightly damaged
1.29	0.8	Damaged
2.10	1.5	Damaged
2.75	1.8	Damaged
4.36	2.2	Damaged

Table 3-2: Measurements of laser exposure on ex-vivo rabbit corneas (frozen) at 2.7 μm

Radiant exposure (J/cm^2)	Temperature change (^oC)	Cornea status
0.40	0	Undamaged
0.65	0.3	Undamaged
0.75	0.5	Undamaged
0.89	0.7	Slightly damaged
1.29	0.9	damaged
2.15	1.1	damaged
2.83	1.6	damaged
4.52	2.2	damaged

3.3 Ex-vivo rabbit eye measurements at 2.5 μm

Laser radiation exposure on both fresh and frozen rabbit eyes has been performed at 2.5 μm using methods similar to that at 2.7 μm. Due to the change of index of refraction of the magnesium fluoride lens at different wavelengths, the beam size at exactly the same location behind the lens for a 2.5 μm laser beam is about 15-20% less than that for 2.7 μm. Therefore, even with the same amount of laser output energy, the radiant exposure on the cornea was about 40% higher at 2.5 μm than that at 2.7 μm.

Results of the laser irradiation on fresh and frozen rabbit eyes at 2.5 μm are shown in Figures 3-7 and 3-8, respectively. Similar to the observations at 2.7 μm, fresh and frozen rabbit eyes did not behave significantly different from one another at a specific laser radiant exposure. In addition, for each specified radiant exposure, the pattern of the temperature on the corneal surface was also similar to that observed at 2.7 μm. For example, the temperature on the corneal surface first rose rapidly then decayed back to the initial temperature (baseline) for each measurement in both Figures 3-7, and 3-8, and the temperature changes on the corneal surfaces as well as the temperature recovery time were proportional to the incident radiant exposures. A maximum

temperature change of 3.0 ^{o}C at the available maximum radiant exposure (~ 9.11 J/cm^2) at 2.5 μm was observed, and both fresh and frozen rabbit eyes were damaged at a similar exposure (first observed at 3.9 J/cm^2) with an indicated temperature change of 1.0 – 1.1 ^{o}C.

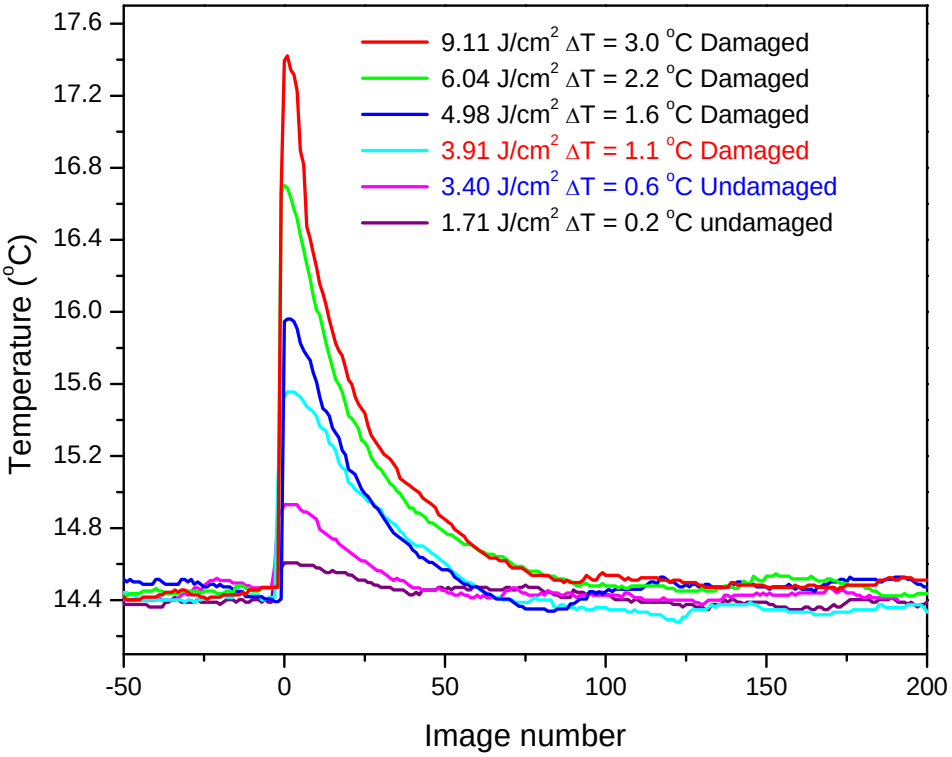

Figure 3-7: Measurements of laser radiation exposure on fresh rabbit eyes at 2.5 μm.

However, by comparing the measurements at both wavelengths, a major difference was found. Much higher radiant exposure was required at 2.5 μm than at 2.7 μm to produce a similar biological effect, such as temperature change and lesion on the cornea. For instance, at 2.7 μm the first observable lesion was induced at a radiant exposure of about 1.29 J/cm^2, which led to a temperature change of 0.8-0.9 ^{o}C on the corneal surface, but it required ~3.9 J/cm^2 at 2.5 μm to cause a similar temperature change, and to cause first observable damage on the cornea. This difference indicates that

the damage threshold of the rabbit cornea is wavelength dependent, and it is greater at 2.5 μm than that at 2.7 μm.

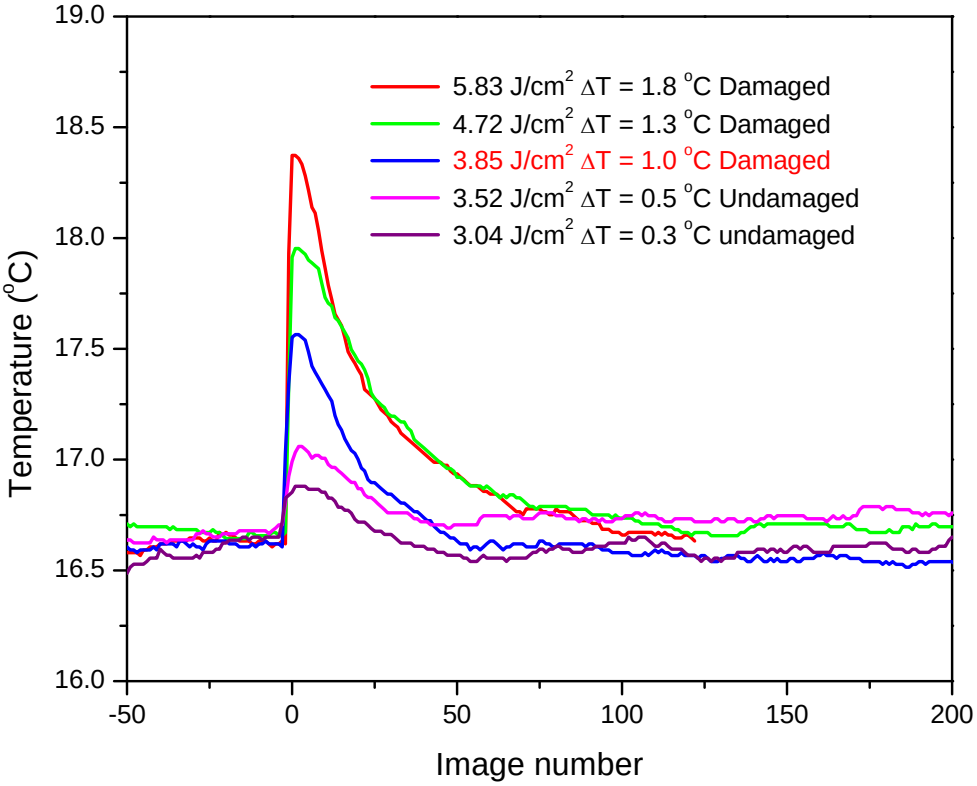

Figure 3-8: Measurements of laser radiation exposure on frozen rabbit eyes at 2.5 μm.

The experimental data for fresh and frozen rabbit eyes at 2.5 μm are listed in Tables 3-3 and 3-4, respectively. For the same reasons as in the measurements at 2.7 μm, some extra measurements were performed to determine damage threshold only. A full list of all measurements with and without temperatures for fresh and frozen rabbit eyes are given in the appendix as tables TA 3-3 and TA3-4. Based on the experimental data listed in these two tables, the ED_{50}s for the laser irradiation on the rabbit cornea at 2.5 μm were determined to be 3.67 and 3.62 J/cm^2 for fresh and frozen eyes, respectively. These values are about 4.5 times higher than at 2.7 μm (0.8 J/cm^2).

Table 3-3: Measurements of laser exposure on ex-vivo rabbit corneas (Fresh) at 2.5 μm

Radiant exposure (J/cm^2)	Temperature change (^oC)	Cornea status
0.62	0	Undamaged
1.03	0	Undamaged
1.22	0	Undamaged
1.71	0.2	Undamaged
1.91	0.4	Undamaged
2.31	0.5	Undamaged
2.98	0.5	Undamaged
3.40	0.6	Undamaged
3.91	1.1	Slightly damaged
4.98	1.6	damaged
6.04	2.2	damaged
9.11	3.0	damaged

Table 3-4: Measurements of laser exposure on ex-vivo rabbit corneas (frozen) at 2.5 μm

Exposure irradiance (J/cm^2)	Temperature change (^oC)	Cornea status
3.04	0.3	Undamaged
3.52	0.5	Undamaged
3.85	1.0	Slightly damaged
4.72	1.3	damaged
5.83	1.8	damaged

3.4 Ex-vivo pig eye measurements

To compare the damage thresholds of the cornea for different animals (rabbit and pig in this work), identical experimental measurements have been performed to determine the laser damage thresholds of pig corneas at both 2.5 and 2.7 μm. Because fresh pig eyes were not available during the experimental measurements, only frozen eyes were measured in this work. Similar to the treatment to frozen rabbit eyes, the frozen pig eyes were also warmed back to ~16 ^{o}C before experimental measurements. The measurements at 2.7 and 2.5 μm are plotted in Figures 3-9 and 3-10, respectively. Both plots indicate that the temperature changes on the pig corneal surfaces are proportional to the incident

radiant exposures, and the temperature recovery time is also dependent on the radiant exposure on the cornea.

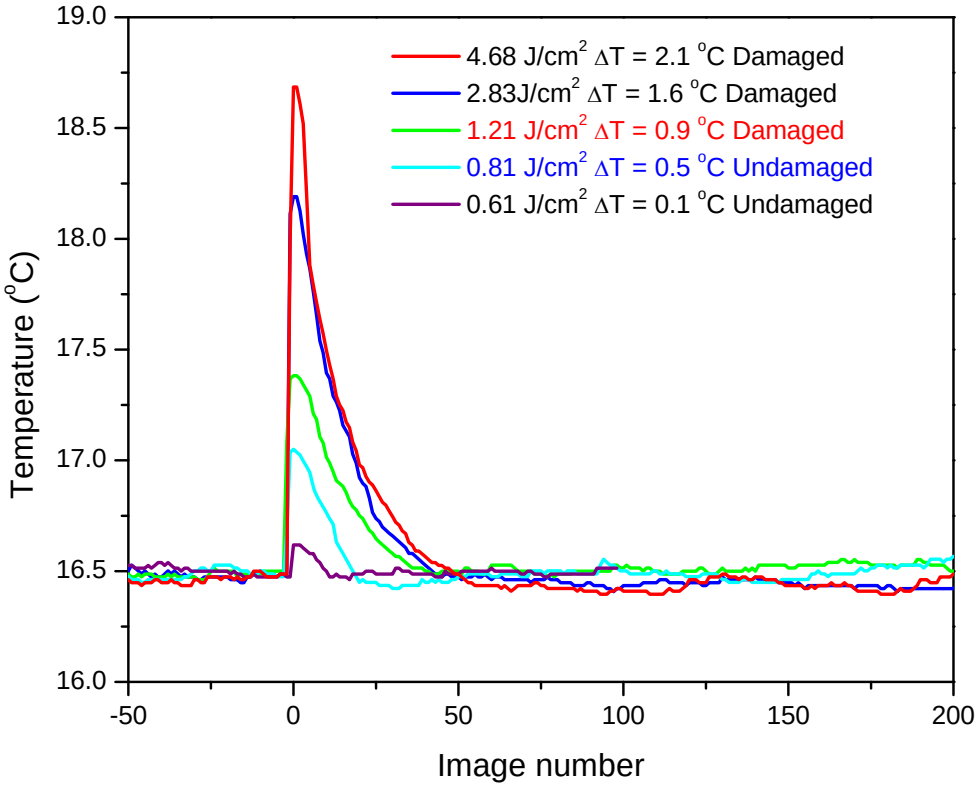

Figure 3-9: Measurements of laser radiation exposure on frozen pig eyes at 2.7 μm.

Figure 3-9 suggests that the laser damage threshold of a pig cornea at 2.7 μm is similar to that of a rabbit cornea at the same wavelength because the radiant exposure that caused damage on the pig cornea, and the temperature change at this radiant exposure are very similar to the measurements for rabbit corneas. In addition, a comparison between Figures 3-9 and 3-10 indicates that the damage threshold of pig cornea at 2.5 μm is greater than at 2.7 μm. This observation is also in a good agreement with that for rabbit corneas.

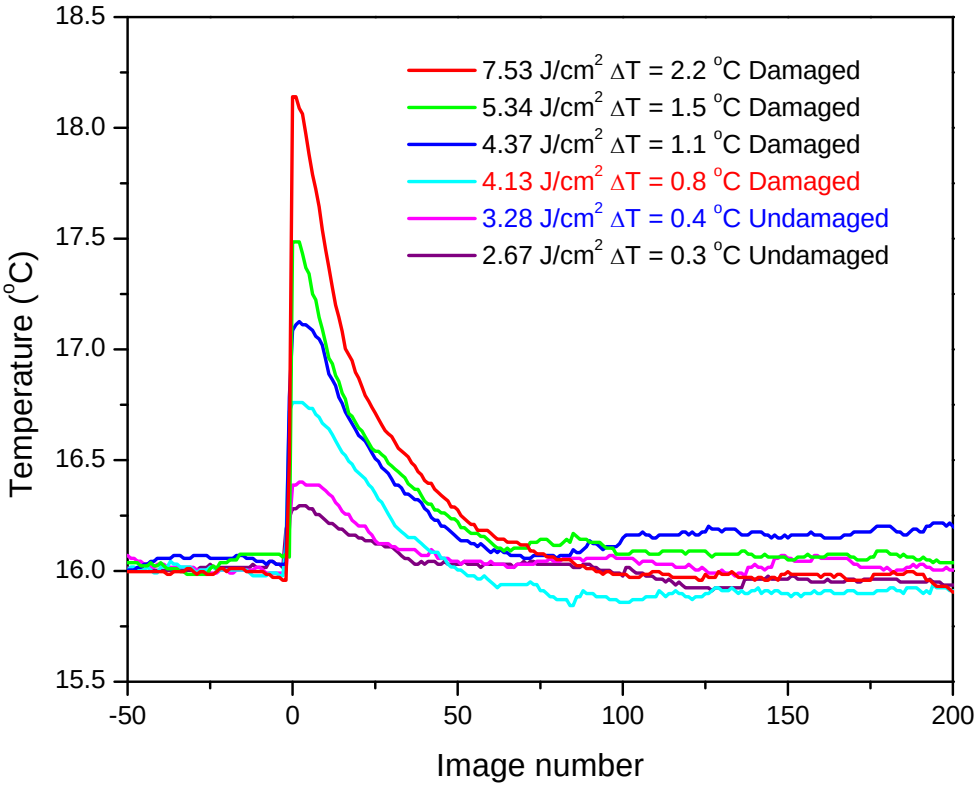

Figure 3-10: Measurements of laser radiation exposure on frozen pig eyes at 2.5 μm.

The experimental data for pig eyes at 2.7 and 2.5 μm are listed in Tables 3-5 and 3-6, respectively. Some extra data to determine the damage threshold was also included in the ED_{50} calculations using a Probit program. The full list of data with and without temperatures for pig eyes at 2.7 and 2.5 μm are given as Tables TA 3-5 and TA3-6, respectively, in the appendix. Based on the experimental data listed in these two tables, the ED_{50}s for the laser irradiation on the pig cornea at 2.5 and 2.7 μm were determined to be 0.88 and 3.68 J/cm^2, respectively. The value at 2.5 μm is about 4.2 times higher than at 2.7 μm.

Table 3-5: Measurements of laser exposure on ex-vivo pig corneas (frozen) at 2.7 μm

Exposure irradiance (J/cm^2)	Temperature change (^oC)	Cornea status
0.61	0.1	Undamaged
0.81	0.5	Undamaged
1.21	0.9	damaged
2.26	1.1	damaged
2.83	1.6	damaged
4.68	2.1	damaged

Table 3-6: Measurements of laser exposures on ex-Vivo pig corneas (frozen) at 2.5 μm

Exposure irradiance (J/cm^2)	Temperature change (^oC)	Cornea status
1.76	0.0	Undamaged
2.06	0.1	Undamaged
2.67	0.3	Undamaged
3.28	0.4	Undamaged
4.13	0.8	damaged
4.37	0.9	damaged
5.34	1.5	damaged
7.53	2.2	damaged

3.6 Summary of ED_{50}s of pig and rabbit corneas

Based on the measurements and calculations mentioned above, the ED_{50}s of laser radiation exposure on pig and rabbit corneas at 2.5 and 2.7 μm are summarized in Table 3-7. The corresponding MPE values are also included in this table [35]. More details on the MPE will be discussed in the next chapter. Uncertainties (1σ) were calculated based on error propagation from standard deviations of energy and beam size measurements.

Table 3-7: Summary of ED_{50}s of pig and rabbit corneas at 2.5 and 2.7 μm

Animal	Type of eyes	Wavelengths (μm)	ED_{50} (J/cm^2)	MPE (J/cm^2)
Rabbit	Fresh	2.7	0.81 ± 0.14	0.01
Rabbit	Frozen	2.7	0.83 ± 0.14	0.01
Rabbit	Fresh	2.5	3.67 ± 0.43	0.1
Rabbit	Frozen	2.5	3.62 ± 0.42	0.1
Pig	Frozen	2.7	0.88 ± 0.14	0.01
Pig	Frozen	2.5	3.68 ± 0.43	0.1

CHAPTER 4: DISCUSSION

4.1 Comparison of laser damage thresholds between fresh and frozen corneas

As mentioned in chapter 3, laser damage thresholds or ED_{50}s of both fresh and frozen rabbit corneas have been measured. Based on Table 3-7, there is no significant difference between fresh and frozen rabbit corneas within the uncertainty of the measurements. The ED_{50}s for fresh and frozen rabbit cornea at 2.7 μm were 0.81 ± 0.14 and 0.83 ± 0.14 J/cm^2, respectively. At 2.5 μm, the ED_{50}s for fresh (3.67 ± 0.43 J/cm^2) and frozen (3.62 ± 0.42 J/cm^2) rabbit corneas were not significantly different either. Therefore, laser interaction with fresh and frozen processed corneal tissues produced similar biological effects, and the freezing process did not change the damage thresholds for 2.5 and 2.7 μm.

A comparison of the damage thresholds (or ED_{50}s) for fresh and frozen rabbit corneas can also be found in Figures 4-1, and 4-2, where the temperature changes on the corneal surfaces were plotted versus radiant exposure at 2.7 and 2.5 μm, respectively. First, both fresh and frozen corneas behave similarly to one another not only at the damage thresholds, but also in the whole available radiant exposure range. Secondly, at both wavelengths (2.7 and 2.5 μm), although the damage thresholds are different from one another, the temperature changes on the corneal surface are similar (0.65 - 0.75 ^{o}C) at the ED_{50}. A temperature threshold for corneal damage is indicated at ~0.7 ^{o}C temperature rise at both 2.7 and 2.5 μm.

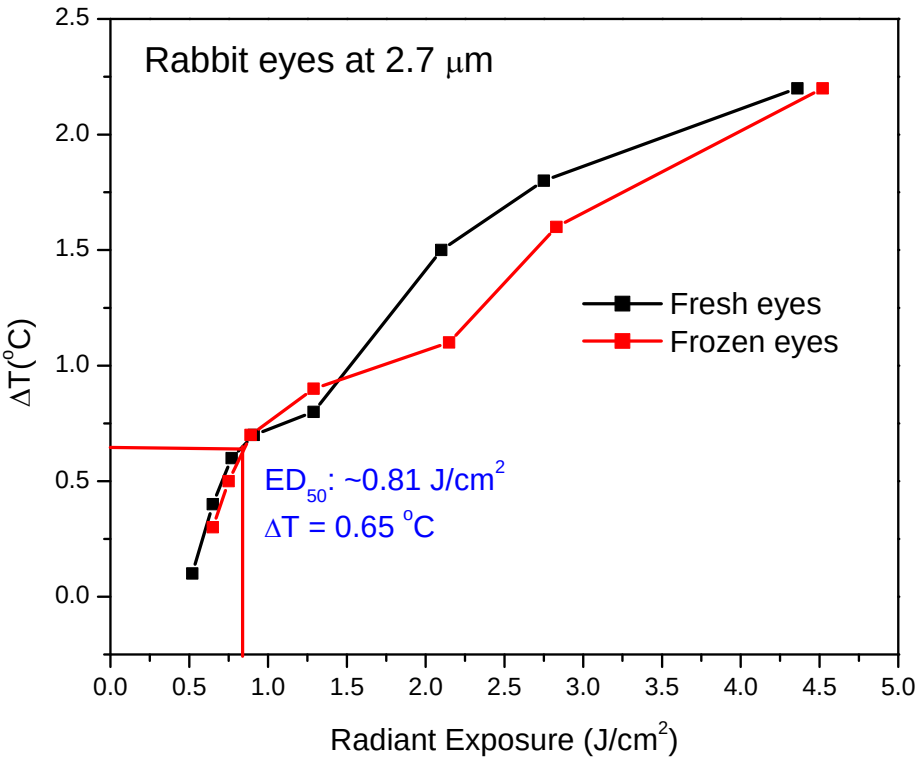

Figure 4-1: Temperature changes on the fresh and frozen processed rabbit corneal surfaces versus radiant exposure at 2.7 μm.

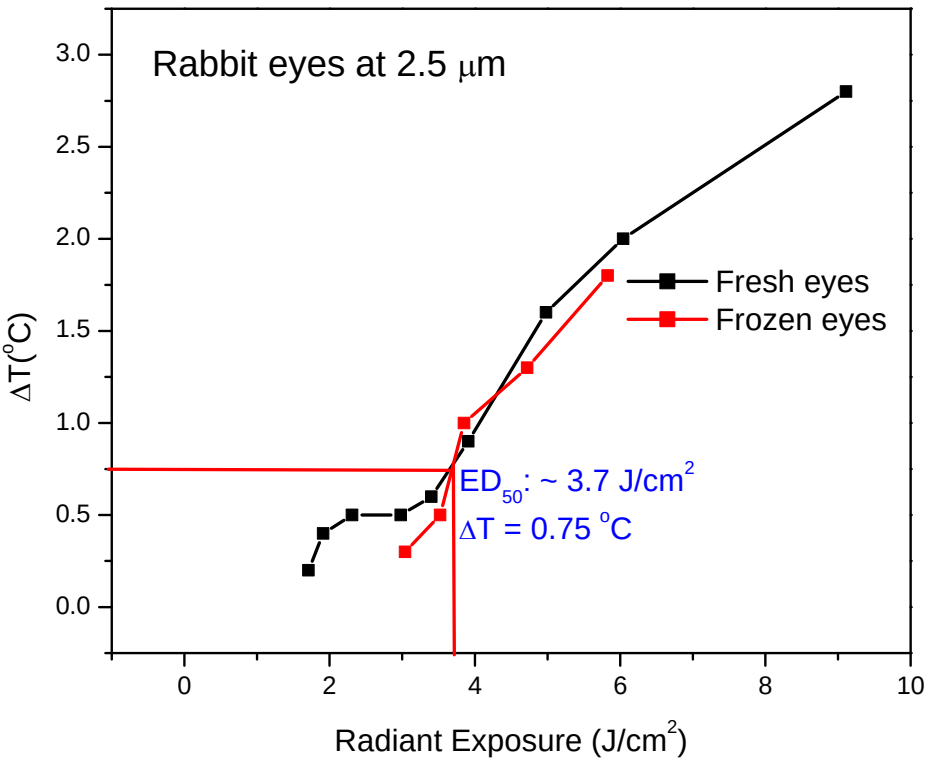

Figure 4-2: Temperature changes on the fresh and frozen processed rabbit corneal surfaces versus radiant exposure at 2.5 μm.

4.2 Comparison of laser damage thresholds between pig and rabbit corneas

The damage thresholds of frozen pig corneas (0.88 J/cm^2 at 2.7 μm, and 3.68 J/cm^2 at 2.5 μm) are similar to that of frozen rabbit corneas (0.83 J/cm^2 at 2.7 μm, and 3.62 J/cm^2 at 2.5 μm). Statistically, pig and rabbit corneas respond in an identical manner. These results indicate that laser interaction with both pig and rabbit corneal tissues appears to be similar, and adds to evidence that these thresholds might be extended to humans. The fact that the damage thresholds of pig and rabbit corneas are consistent further confirms that laser safety standards based on animal studies appear reasonable [18].

4.3 Comparison of laser damage thresholds at 2.7 and 2.5 μm

Because of the smaller beam size at 2.5 μm, if the damage thresholds of rabbit corneas at both wavelengths are similar, we expected that about 40% less laser energy at 2.5 μm would produce similar biological effects to that at 2.7 μm, including temperature change and damage on the corneal surfaces. As a matter of fact, however, it required much higher radiant exposure at 2.5 μm than at 2.7 μm to produce similar biological effects on the rabbit cornea. This means that the damage threshold of the cornea at 2.5 μm should be much greater than that at 2.7 μm. Experimental measurements show that the damage thresholds of both pig and rabbit corneas at 2.5 μm are about 4.2 - 4.5 times higher than at 2.7 μm. In addition, at each laser wavelength, the laser damage thresholds for both pig and rabbit corneas are similar to one another. This suggests that both pig and rabbit corneas might have certain substances or structures in common that play an important role in the IR laser damage. According to previous studies on corneal injury in

the middle IR spectral region [36, 37], the damage to the cornea at high radiant exposure reaches the stromal layer of the cornea, which accounts for 90% of the thickness of the cornea, and 70% of the stromal layer is water. Thus we hypothesize that water is the primary absorber, which determines the damage of the cornea at IR laser radiation exposure. If this assumption is true, then water absorption may play an essential role in the damage caused by IR laser radiation to the cornea of many animal species.

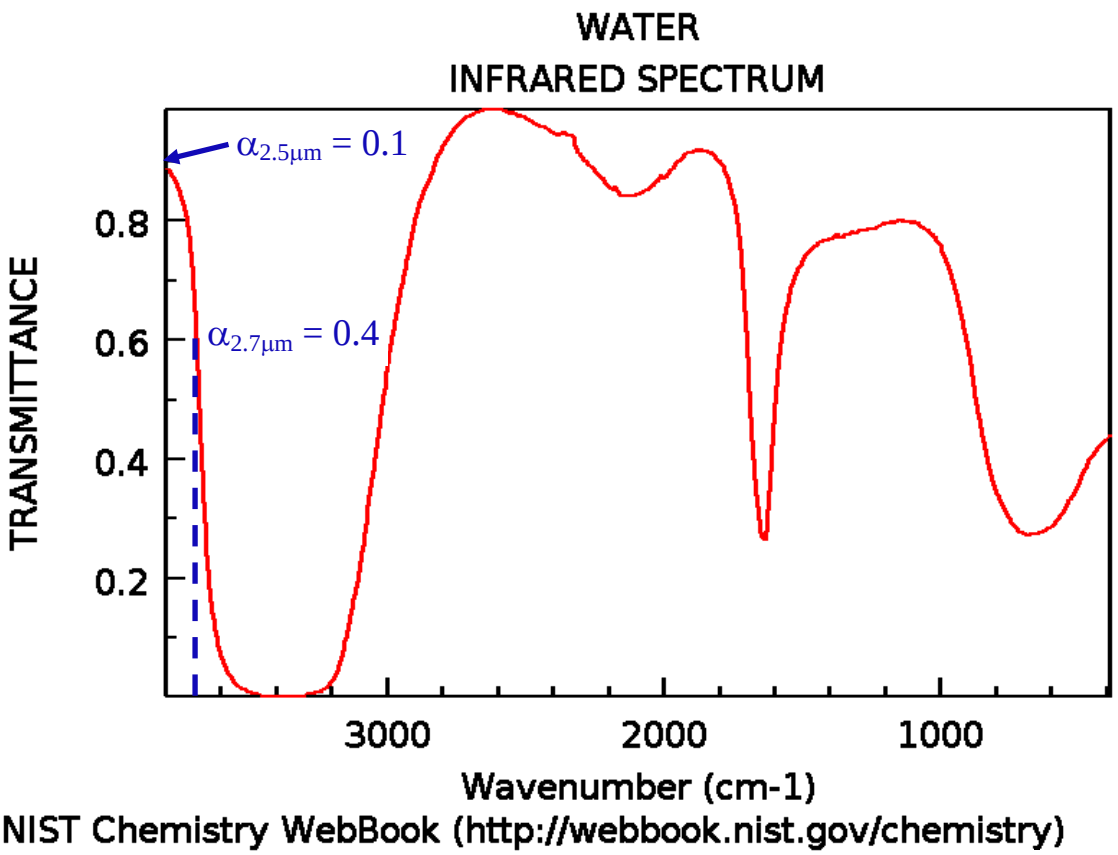

Figure 4-3: Water absorption spectrum at middle IR wavelength range.

The absorption spectrum of liquid water in the middle IR wavelength range is shown in Figure 4-3 [38]. The absorption coefficients for water at 2.7 (3700 cm^{-1}) and 2.5 (4000 cm^{-1}) μm are around 0.4 and 0.1, respectively. The ratio of the absorption coefficients at these two wavelengths is about 4, which is in a good agreement with the

ratio (4.2-4.5) of the ED_{50}s between 2.5 and 2.7 μm. This agreement further implies that water absorption does play an important role in the laser damage of the cornea in the middle IR spectral region. Water has a maximum absorption ($\alpha_{2.9\mu m} = 1$) at about 2.9 μm (3400 cm^{-1}). Thus, if the 2.9 μm wavelength was used to measure the damage thresholds of pig and rabbit corneas, one can roughly estimate the ED_{50} at 2.9 μm to be 0.32 J/cm^2, which is about 2.5 times less than that at 2.7 μm. Due to the lack of proper neutral density filters for the 2.9 μm wavelength in our lab, the experimental measurements at this wavelength was not performed.

Muller and co-workers have measured the ED_{50} for rabbit cornea at 2.9 μm with 100 ns laser pulse duration and 2 cm^2 beam size [32]. They determined the ED_{50} to be 6.99 J/cm^2, which is about 20 times higher than the value (0.32 J/cm^2) estimated in this work. The possible reason for this large difference might be the difference in the laser pulse duration, or the difference in the beam size, or both. However, it is more likely that the difference is caused by the different laser pulse duration employed between these two experiments because the ratio of the time duration is about 12 (100/8), but the ratio of the beam size is about 1667 (200/0.12). Nevertheless, this statement is based on the assumption that the corneal response is directly proportional to either the time duration or the beam size. Laser pulse duration has been shown to be another important factor in the determination of the damage threshold of the cornea by Dunsky and Egbert, who observed that the damage thresholds of the rheasus monkey's cornea decreased with decreasing laser pulse duration [31].

4.4 Significance of temperature measurements on the corneal surface

In this work, the damage thresholds of the pig and rabbit corneas were determined, as well as the temperature changes on the corneal surfaces were recorded. Based on experimental measurements, at both 2.5 and 2.7 μm, the temperature changes on the corneal surfaces were about 0.7 ^{o}C at the ED_{50} radiant exposure. This temperature change is relatively low compared to a recent measurement performed in our lab, in which a 2.1 μm laser with pulse duration of 10 ms was employed, and a temperature change of 8.3 ^{o}C was observed at a radiant exposure of 2.8 J/cm^2 without damage to the cornea [39].

The possible reason for this big difference might be due to the large difference in the laser pulse duration used in these two measurements. With a short laser pulse duration, a high power density (1 - 5 × 10^8 W/cm^2) can be easily reached, causing a high probability of multi photon absorption, which results in tissue damage by highly localized energy absorption (or photo ablation) instead of by thermal injury. Therefore, the indicated temperature on the cornea did not change too much even when the tissue was damaged. A second concern is the accuracy of the temperature measurement. The thermal camera had only ms time resolution and was employed to monitor the temperature change caused by a laser radiation exposure within 8 ns time duration. In this case, the maximum temperature change might be missed by the camera, causing an incorrect reading of the measured temperature. However, experimentally the observed temperature fluctuation was primarily caused by laser output energy instability (partial fluctuation might own to the relatively low resolution of the camera), as shown in Figure 3-4, and the temperature change on the corneal surface was proportional to the laser radiant exposure.

Therefore, the temperature monitoring in this work appears to be valid for the surface of the cornea, and the small temperature change (0.7 ^{o}C) at the ED_{50} irradiation exposure with short time duration is a useful and significant measurement for reference. Most likely, the actual peak temperatures may have been at a depth that could not be measured by the IR camera. Further research is needed to determine where in the depth profile these photons are absorbed and if the multiphoton effect has an impact on IR camera temperature measurements.

4.5 Recommended MPE at 2.5 and 2.7 μm wavelengths

The recommended MPEs for 2.5 and 2.7 μm laser wavelengths with ns pulse duration are 0.1 and 0.01 J/cm^2 [35], respectively. These values are listed in Table 3-7 for comparison. Clearly, both the recommended MPEs and the measured ED_{50}s show strong wavelength dependence. More interestingly, the two wavelengths used in this work are located in two separate wavelength ranges (1.8 -2.6 μm, and 2.6 -1000 μm) where a step function of the MPE is defined. In addition, one can find that the recommended MPEs at 2.5 and 2.7 μm are about 35 and 80 times, respectively, below the measured damage thresholds at these wavelengths. Therefore, we conclude that the recommended MPEs at these wavelengths are overly conservative.

4.6 Future works

The current work focuses primarily on the measurements of damage thresholds of pig and rabbit corneas at 2.5 and 2.7 μm. Based on the determined ED_{50}s at these two wavelengths, the damage thresholds of the cornea in the middle IR spectral region were strongly wavelength dependent and possibly affected by water absorption. One interesting work for the future is to measure the damage thresholds of cornea at other

wavelengths where water absorption changes rapidly, such as 2.6, 2.8 and 2.9 μm, and so on. This way one can eventually plot the ED_{50}s versus wavelength, and determine if the plot is consistent with the liquid absorption spectrum at these wavelengths. The results from this future work would provide complete information about the role of water absorption in the IR laser damage of the cornea, and make it possible to extrapolate the ED_{50}s for wavelengths that have not been measured based on the relative water absorption at these wavelengths.

This study also suggests that the laser pulse duration could be another critical parameter in the determination of ED_{50}s of the cornea. The shorter the laser pulse duration, the lower the damage threshold of the cornea. With the rapid development and application of ultrafast lasers, it becomes increasingly important to establish reliable laser safety standard for the ultrafast region. Therefore, another future work, as an extension of this study, could be measurements of the damage threshold of the cornea in the middle IR spectral region with pico-, femto-, and even atto- second time duration.

CHAPTER 5: SUMMARY AND CONCLUSIONS

5.1 Summary

With the rapid expansion of laser applications in all kinds of new fields, especially some fields directly involving the public, the establishment of reliable laser safety standards becomes more and more important. In this work, we have focused our effort on the measurement of laser damage thresholds of the cornea using both ex-vivo pig and rabbit models at middle IR wavelengths. Since the bulk of the cornea is water, the role of the water absorption in the damage of the cornea has been examined via the comparison of damage thresholds of the cornea at different wavelengths with different water absorption coefficients. Experimental measurements demonstrate that the damage thresholds of the cornea are inversely proportional to the water absorption coefficients. Additionally, the laser damage threshold of the cornea from short pulse durations (8 ns) provides important information about the time duration dependence of the damage thresholds of the cornea, especially in nanosecond and picoseconds time scales where multi photon absorption may be important.

Laser radiation exposure on fresh and frozen eyes has been examined to determine if the freezing process changed the characteristics of the corneal structure in the context of damage threshold determination. Experimentally, no significant difference was observed between the fresh and the frozen corneas. Moreover, the studies of the damage threshold of the cornea of pig and rabbit eyes provide evidence for the possibility of an extension of the results to humans.

5.2 Conclusions

Laser damage thresholds (ED_{50}s) of pig and rabbit corneas at 2.7 and 2.5 μm were found to be 0.8 and 3.7 J/cm^2, respectively. The damage threshold of pig corneas is similar to that of rabbit corneas. The essential role of the water absorption in the damage of the cornea was confirmed by the different damage thresholds at 2.7 and 2.5 μm wavelengths. The ED_{50}s for both wavelengths were much greater than the corresponding recommended MPEs. Current MPEs appear overly restrictive, and a revision of the laser safety standard at those wavelengths with short pulse durations may be necessary.

REFERENCES

1. T. Maiman, Optical and microwave-optical experiments in ruby, Phys. Rev. Lett. 4, 564-566, 1960.

2. J. F. Ready, Industry applications of laser, 2nd ed., Academic Press, 1997.

3. Y. Tang, J. Y. Fuh, H. T. Loh, Y. S. Wong, and Y. K. Lim, Laser dicing of silicon wafer, Surface Rev. and Letts, 15, 153-159, 2008.

4. Vogel, A. and Venugopalan V. Mechanisms of pulsed laser ablation of biological tissues, Chem. Rev. 103, 577, 2003.

5. J. A. Dixon, Current application of laser in general surgery, Ann. Surg., 201, 355-372, 1988.

6. D. Casasent, Recyclable input devices and special filter materials for coherent optical processing, Laser appl., 3, 43-103, 1977.

7. W. Demtroder, Laser spectroscopy: Basic concept and instrumentation, 3rd ed., Springer, New York, 2003.

8. J. A. McCray, and P. D. Smith, Application of laser to molecular biology, Laser Appl., 3, 1-39, 1977.

9. D. Sliney, and M. Wolbarsht, Safety with Lasers and other Optical Sources, Plenum, New York, 1980.

10. ACIGH, American Conference of Governmental Industrial Hygienists, A guide for Control of Laser Hazards, Cincinnati, 1968.

11. ANSI, American National Standards Institute, Safe Use of Lasers, Standard Z-136.1, New York, 1976.

12. Occupational Safety and Health Administration, "Guidelines for laser safety and hazard assessment," Report STD 01-05-001 [Pub 8-1-7], 1991.

13. M. H. Niemz, Laser-Tissue Interactions: Fundamentals and applications, 3rd ed. Springer, 2004.

14. W. J. Geeraets, E. R. Berry, Ocular spectral characteristic as related to hazards from laser and other light sources, Amer. J. Ophthal. 66, 15-20, 1968.

15. A. Vassililiadis, Ocular damage from laser radiation, In: Wolbarsht, M. L., ed. Laser applications in medicine and biology, Vol. I. New York: Plenum Press; 1971, 125-162.

16. International Commission on Non-Ionizing Radiation Protection, Guidelines on limits of exposure to laser radiation of wavelengths between 180 nm and 1000 μm, Health Phys., 71, 804-819, 1996.

17. J. G. Fyffe, T. A. Neal, W. P. Bulter, and T. E. Johnson, The Ex vivo pig eye as a replacement model for laser safety testing, Comparative Medicine, 55, 503-509, 2005.

18. C. B. Bargeron, R. A. Farrell, W. R. Green, and R. L. McCally, Corneal damage from exposure to IR radiation: rabbit endothelial damage thresholds, Health Physics, 40, 855-862, 1981.

19. American National Standard Institute, American National Standard recommended practices for laser safety measurements for hazard evaluation (ANSI Z136.4-2005) Laser Institute of America, Inc., Orlando, Fla., 2005.

20. D. Sliney, J. Mellerio, V. P. Gabel, and K. Schulmeister, What is the meaning of threshold in laser injury experiments? Implications for human exposure limits, Health Phys. 82, 335-347, 2002.

21. W. T. Ham, H. A. Muller, and D. H. Sliney, Retina sensitivity to damage from short wavelength light, Nature, 260, 153-155, 1976.

22. W. K. Noell, Possible mechanisms of photoreceptor damage by light in mammalian eyes, Vision Res. 20, 1163-1171, 1980.

23. D. Courant, L. Court, B. Abadie, and B. Brouillet, Retinal damage thresholds from single-pulse laser exposures in the visible spectrum, Health Phys., 56, 637-642, 1989.

24. J. Marshall, Eye hazards associated with laser, Ann. Occup. Hyg., 21, 69-77, 1978.

25. J. J. M. Kremers, and D. Van Norren, Two classes of photochemical damage of the retina, Laser and Light in Ophthalmol., 2, 41-52, 1988.

26. A. S. Brownell, B. E. Stuck, Ocular and Skin Hazards from CO2 laser radiation, Proc. 9th Army Sci. Conf., June, 1974.

27. B. S. Fine, S. Fine, G. R. Peacock, W. J. Geeraets, and E, Klein, Preliminary observations on ocular effects of high power, continuous CO2 laser irradiation, Am. J. Ophthal., 64, 209, 1967.

28. N. A. Peppers, A. Vassiliadis, K. G. Dedrick, H. Vhang, R. R. Peabody, H. Rose, and H. C. Zweng, Cornea damage thresholds for CO2 Laser radiation, Appl. Optics, 8, 377, 1969.

29. M. A. Mainster, Ophthalmic applications of infrared lasers-Thermal considerations, Invest. Ophthalmol. Visual Sci., 18, 414, 1979.

30. C. B. Bargeron, R. L. McCally, R. A. Farrell, Calculated and measured endothelia temperature histories of excited rabbit corneas exposed to infrared radiation, Experimental Eye Res., 37, 543-550, 1981.

31. I. L. Dunsky, and D. E. Egbert, Corneal damage thresholds for hydrogen fluoride and deuterium fluoride chemical lasers, p. 1-28. U.S.A.F. School of Aerospace Medicine, San Antonio, Tex., 1972.

32. H. A. Muller, W. T. Ham, The Ocular effects of single pulses of 10.6 μm and 2.5-3.0 μm Q-switched laser radiation, p. 1-18. In A report to the Los Alamos scientific laboratory L-division. Department of Biophysics, Health Sciences Division, Virginia Commonwealth University, Richmond, VA.

33. E. F. Maher, Transmission and absorption coefficients for ocular media of the rhesus monkey, p. 102. U.S.A.F. School of Aerospace Medicine, San Antonio, Tex., 1972.

34. D. J. Finney, Probit analysis, 3rd ed. Cambridge University Press, Cambridge, 1971.

35. American National Standards Institute, "American national standard for safe use of lasers," Report No. ANSI Z136.1-2007, 2007.

36. B. E. Stuck, D. J. Lund, and E. S. Beatrice, Ocular effects of holmium (2.06 μm) and erbium (1.54 μm)laser radiation. Health Phys., 40, 835-846, 1981.

37. R. L. McCally, R. A. Farrell, and C. B. Bargeron, Cornea epithelial damage thresholds in rabbits exposed to Tm:YAG laser radiation at 2.02 μm. Laser Surg. Med., 12, 598-603, 1992.

38. Smith, A.L., The Coblentz Society Desk Book of Infrared Spectra in Carver, C.D., editor, The Coblentz Society Desk Book of Infrared Spectra, Second Edition, The Coblentz Society:Kirkwood, MO, p. 1-24, 1982.

Appendix A

TA3-1: Measurements of laser exposure on ex-vivo rabbit corneas (Fresh) at 2.7 μm

Exposure irradiance (J/cm^2)	Temperature change (^oC)	Cornea status
0.52	0.1	Undamaged
0.65	0.4	Undamaged
0.77	0.6	Undamaged
0.91	0.7	Slightly damaged
1.29	0.8	Damaged
2.10	1.5	Damaged
2.75	1.8	Damaged
4.36	2.2	Damaged
0.40	N/A	Undamaged
0.40	N/A	Undamaged
0.43	N/A	Undamaged
0.60	N/A	Undamaged
0.64	N/A	Undamaged
0.73	N/A	Undamaged
0.74	N/A	Undamaged
0.76	N/A	Undamaged
0.86	N/A	Slightly damaged
0.93	N/A	Damaged
0.97	N/A	Damaged
1.05	N/A	Damaged
1.05	N/A	Damaged
1.41	N/A	Damaged
1.45	N/A	Damaged
1.45	N/A	Damaged
2.10	N/A	Damaged
2.25	N/A	Damaged
2.34	N/A	Damaged
2.34	N/A	Damaged
2.82	N/A	Damaged
2.90	N/A	Damaged
2.91	N/A	Damaged
2.95	N/A	Damaged
4.43	N/A	Damaged
4.75	N/A	Damaged
4.88	N/A	Damaged

Appendix A

TA 3-2: Measurements of laser exposure on ex-vivo rabbit corneas (Frozen) at 2.7 μm

Exposure irradiance (J/cm^2)	Temperature change (^oC)	Cornea status
0.40	0	undamaged
0.65	0.3	Undamaged
0.75	0.5	Undamaged
0.89	0.7	Slightly damaged
1.29	0.9	damaged
2.15	1.1	damaged
2.83	1.6	damaged
4.52	2.2	damaged

Appendix A

TA 3-3: Measurements of laser exposure on ex-vivo rabbit corneas (Fresh) at 2.5 μm

Exposure irradiance (J/cm^2)	Temperature change (^oC)	Cornea status
0.62	0	Undamaged
1.03	0	Undamaged
1.22	0	Undamaged
1.71	0.2	Undamaged
1.91	0.4	Undamaged
2.31	0.5	Undamaged
2.98	0.5	Undamaged
3.40	0.6	Undamaged
3.91	1.1	Slightly damaged
4.98	1.6	damaged
6.04	2.2	damaged
9.11	3.0	damaged
0.60	N/A	Undamaged
1.05	N/A	Undamaged
1.12	N/A	Undamaged
1.22	N/A	Undamaged
1.78	N/A	Undamaged
1.82	N/A	Undamaged
2.02	N/A	Undamaged
2.38	N/A	Undamaged
2.38	N/A	Undamaged
3.04	N/A	Undamaged
3.14	N/A	damaged
4.02	N/A	damaged
4.80	N/A	damaged
4.81	N/A	damaged
5.97	N/A	damaged
6.09	N/A	damaged
9.14	N/A	damaged
9.26	N/A	damaged

Appendix A

TA 3-4: Measurements of laser exposure on ex-vivo rabbit corneas (Frozen) at 2.5 μm

Exposure irradiance (J/cm^2)	Temperature change (^oC)	Cornea status
3.04	0.3	Undamaged
3.52	0.5	Undamaged
3.85	1.0	Slightly damaged
4.72	1.3	damaged
5.83	1.8	damaged
1.04	N/A	Undamaged
1.21	N/A	Undamaged
1.72	N/A	Undamaged
1.77	N/A	Undamaged
2.01	N/A	Undamaged
2.36	N/A	Undamaged
3.39	N/A	Undamaged

Appendix A

TA 3-5: Measurements of laser exposure on ex-vivo pig corneas (Frozen) at 2.7 μm

Exposure irradiance (J/cm^2)	Temperature change (^oC)	Cornea status
0.61	0.1	Undamaged
0.81	0.5	Undamaged
1.21	0.9	damaged
2.26	1.1	damaged
2.83	1.6	damaged
4.68	2.1	damaged
0.40	N/A	Undamaged
0.64	N/A	Undamaged
0.97	N/A	damaged
0.97	N/A	damaged
1.45	N/A	damaged
2.62	N/A	damaged
2.62	N/A	damaged
2.83	N/A	damaged
4.76	N/A	damaged

TA 3-6: Measurements of laser exposures on ex-vivo pig corneas (Frozen) at 2.5 μm

Exposure irradiance (J/cm^2)	Temperature change (^oC)	Cornea status
1.52	0.0	Undamaged
1.76	0.0	Undamaged
2.06	0.1	Undamaged
2.67	0.3	Undamaged
3.28	0.4	Undamaged
4.13	0.8	damaged
4.37	0.9	damaged
5.34	1.5	damaged
7.53	2.2	damaged

Appendix B

O-1: Output of Probit calculation for measurements of fresh rabbit eyes at 2.7 μm

ONES = 16 ZEROES = 8
h = 0.00
g = 0.000
t = 1.960
Percent confidence = 0.95
SYY = 0.000
SXY = 0.000
SXX = 0.000
S0 = 0.000
ED50 = 8.1314e-001
FLU = 8.1314e-001
FLL = 8.1314e-001
Pearson's Chi-Sq = 0.0000 Probability of Chi-Sq = 1.0000
Log XBAR = -0.0890
Log YBAR = 5.1725
Intercept = 18.4283
Slope = 205.1397
Iterations = 22

Prob	Dose	Lower Limit	Upper Limit
0.01	7.9218e-001	- -	
0.02	7.9461e-001	- -	
0.03	7.9616e-001	- -	
0.04	7.9732e-001	- -	
0.05	7.9827e-001	- -	
0.06	7.9908e-001	- -	
0.07	7.9978e-001	- -	
0.08	8.0042e-001	- -	
0.09	8.0100e-001	- -	
0.10	8.0153e-001	- -	
0.15	8.0374e-001	-	-
0.20	8.0550e-001	-	-
0.25	8.0701e-001	-	-
0.30	8.0837e-001	-	-
0.35	8.0963e-001	-	-
0.40	8.1083e-001	-	-
0.45	8.1200e-001	-	-
0.50	8.1314e-001	-	-
0.55	8.1429e-001	-	-
0.60	8.1546e-001	-	-
0.65	8.1667e-001	-	-

0.70	8.1794e-001	-	-
0.75	8.1932e-001	-	-
0.80	8.2086e-001	-	-
0.85	8.2266e-001	-	-
0.90	8.2492e-001	-	-
0.91	8.2547e-001	-	-
0.92	8.2607e-001	-	-
0.93	8.2672e-001	-	-
0.94	8.2746e-001	-	-
0.95	8.2830e-001	-	-
0.96	8.2928e-001	-	-
0.97	8.3049e-001	-	-
0.98	8.3211e-001	-	-
0.99	8.3466e-001	-	-

Dose	Tries	Hits
3.9516e-001	1	0
4.0323e-001	1	0
4.2742e-001	1	0
6.0484e-001	1	0
6.3710e-001	1	0
7.4194e-001	1	0
7.5806e-001	1	0
7.6613e-001	1	0
8.6290e-001	1	1
9.6774e-001	1	1
1.0484e+000	2	2
1.4113e+000	1	1
1.4516e+000	2	2
2.2581e+000	1	1
2.3387e+000	2	2
2.9032e+000	1	1
2.9113e+000	1	1
2.9516e+000	1	1
4.7581e+000	2	2
4.8790e+000	1	1
	24	16

**********Original Data**********

0.39516	0	0.40323	0	0.42742	0	0.60484	0
0.6371	0	0.74194	0	0.75806	0	0.76613	0
0.8629	1	0.96774	1	1.04839	1	1.04839	1
1.41129	1	1.45161	1	1.45161	1	2.25806	1
2.33871	1	2.33871	1	2.90323	1	2.91129	1
2.95161	1	4.75806	1	4.75806	1	4.87903	1

Appendix B

O-2: Output of Probit Calculation for measurements of frozen rabbit eyes at 2.7 μm

ONES = 5 ZEROES = 3
h = 0.00
g = 0.000
t = 1.960
Percent confidence = 0.95
SYY = 0.000
SXY = 0.000
SXX = 0.000
S0 = 0.000
ED50 = 8.2556e-001
FLU = 8.2556e-001
FLL = 8.2556e-001
Pearson's Chi-Sq = 0.0000 Probability of Chi-Sq = 1.0000
Log XBAR = -0.0831
Log YBAR = 5.0227
Intercept = 16.8123
Slope = 201.9416
Iterations = 27

Prob	Dose	Lower Limit	Upper Limit
0.01	8.0395e-001	- -	
0.02	8.0645e-001	- -	
0.03	8.0804e-001	- -	
0.04	8.0924e-001	- -	
0.05	8.1022e-001	- -	
0.06	8.1105e-001	- -	
0.07	8.1178e-001	- -	
0.08	8.1244e-001	- -	
0.09	8.1303e-001	- -	
0.10	8.1358e-001	- -	
0.15	8.1586e-001	-	-
0.20	8.1767e-001	-	-
0.25	8.1923e-001	-	-
0.30	8.2063e-001	-	-
0.35	8.2194e-001	-	-
0.40	8.2318e-001	-	-
0.45	8.2437e-001	-	-
0.50	8.2556e-001	-	-
0.55	8.2674e-001	-	-
0.60	8.2794e-001	-	-
0.65	8.2919e-001	-	-

0.70	8.3051e-001	-	-
0.75	8.3193e-001	-	-
0.80	8.3352e-001	-	-
0.85	8.3537e-001	-	-
0.90	8.3771e-001	-	-
0.91	8.3827e-001	-	-
0.92	8.3889e-001	-	-
0.93	8.3957e-001	-	-
0.94	8.4032e-001	-	-
0.95	8.4119e-001	-	-
0.96	8.4220e-001	-	-
0.97	8.4345e-001	-	-
0.98	8.4512e-001	-	-
0.99	8.4775e-001	-	-

Dose	Tries	Hits
4.0379e-001	1	0
5.2493e-001	1	0
7.6720e-001	1	0
8.8834e-001	1	1
1.2921e+000	1	1
2.1482e+000	1	1
2.8265e+000	1	1
4.5225e+000	1	1
	8	5

**********Original Data**********

0.40379	0	0.52493	0	0.7672	0	0.88834	1
1.29213	1	2.14816	1	2.82653	1	4.52245	1

Appendix B

O-3: Output of Probit calculation for measurements of fresh rabbit eyes at 2.5 μm

ONES = 11 ZEROES = 19
h = 0.00
g = 0.000
t = 1.960
Percent confidence = 0.95
SYY = 0.000
SXY = 0.000
SXX = 0.000
S0 = 0.000
ED50 = 3.6557e+000
FLU = 3.6557e+000
FLL = 3.6557e+000
Pearson's Chi-Sq = 0.0000 Probability of Chi-Sq = 1.0000
Log XBAR = 0.5613
Log YBAR = 4.6660
Intercept = -114.0779
Slope = 202.6362
Iterations = 26

Prob	Dose	Lower Limit	Upper Limit
0.01	3.5603e+000	- -	
0.02	3.5714e+000	- -	
0.03	3.5784e+000	- -	
0.04	3.5837e+000	- -	
0.05	3.5880e+000	- -	
0.06	3.5917e+000	- -	
0.07	3.5949e+000	- -	
0.08	3.5978e+000	- -	
0.09	3.6004e+000	- -	
0.10	3.6028e+000	- -	
0.15	3.6129e+000	-	-
0.20	3.6209e+000	-	-
0.25	3.6278e+000	-	-
0.30	3.6340e+000	-	-
0.35	3.6397e+000	-	-
0.40	3.6452e+000	-	-
0.45	3.6505e+000	-	-
0.50	3.6557e+000	-	-
0.55	3.6609e+000	-	-
0.60	3.6662e+000	-	-
0.65	3.6717e+000	-	-

0.70	3.6775e+000	-	-
0.75	3.6838e+000	-	-
0.80	3.6908e+000	-	-
0.85	3.6990e+000	-	-
0.90	3.7093e+000	-	-
0.91	3.7118e+000	- -	
0.92	3.7145e+000	- -	
0.93	3.7175e+000	- -	
0.94	3.7208e+000	- -	
0.95	3.7247e+000	- -	
0.96	3.7291e+000	- -	
0.97	3.7347e+000	- -	
0.98	3.7420e+000	- -	
0.99	3.7536e+000	- -	

Dose	Tries	Hits
5.9756e-001	1	0
6.2195e-001	1	0
1.0366e+000	1	0
1.0488e+000	1	0
1.1220e+000	1	0
1.2195e+000	2	0
1.7195e+000	1	0
1.7805e+000	1	0
1.8293e+000	1	0
1.9146e+000	1	0
2.0244e+000	1	0
2.3171e+000	1	0
2.3781e+000	2	0
2.9878e+000	1	0
3.0488e+000	1	0
3.1463e+000	1	0
3.4146e+000	1	0
3.9146e+000	1	1
4.0244e+000	1	1
4.8049e+000	1	1
4.8171e+000	1	1
5.0000e+000	1	1
5.9756e+000	1	1
6.0610e+000	1	1
6.0976e+000	1	1
9.1463e+000	2	2
9.2683e+000	1	1
	30	11

**********Original Data**********

0.59756	0	0.62195	0	1.03659	0	1.04878	0
1.12195	0	1.21951	0	1.21951	0	1.71951	0
1.78049	0	1.82927	0	1.91463	0	2.02439	0
2.31707	0	2.37805	0	2.37805	0	2.9878	0
3.04878	0	3.14634	0	3.41463	0	3.91463	1
4.02439	1	4.80488	1	4.81707	1	5	1
5.97561	1	6.06098	1	6.09756	1	9.14634	1
9.14634	1	9.26829	1				

Appendix B

O-4: Output of Probit calculation for measurements of frozen rabbit eyes at 2.5 μm

ONES = 4 ZEROES = 8
h = 0.00
g = 0.000
t = 1.960
Percent confidence = 0.95
SYY = 0.000
SXY = 0.000
SXX = 0.000
S0 = 0.000
ED50 = 3.6170e+000
FLU = 3.6170e+000
FLL = 3.6170e+000
Pearson's Chi-Sq = 0.0000 Probability of Chi-Sq = 1.0000
Log XBAR = 0.5564
Log YBAR = 4.5887
Intercept = -114.7653
Slope = 205.5429
Iterations = 22

Prob	Dose	Lower Limit	Upper Limit
0.01	3.5240e+000	- -	
0.02	3.5348e+000	- -	
0.03	3.5416e+000	- -	
0.04	3.5468e+000	- -	
0.05	3.5510e+000	- -	
0.06	3.5546e+000	- -	
0.07	3.5577e+000	- -	
0.08	3.5605e+000	- -	
0.09	3.5631e+000	- -	
0.10	3.5655e+000	- -	
0.15	3.5753e+000	-	-
0.20	3.5831e+000	-	-
0.25	3.5898e+000	-	-
0.30	3.5958e+000	-	-
0.35	3.6014e+000	-	-
0.40	3.6068e+000	-	-
0.45	3.6119e+000	-	-
0.50	3.6170e+000	-	-
0.55	3.6221e+000	-	-
0.60	3.6273e+000	-	-
0.65	3.6327e+000	-	-

0.70	3.6383e+000	-	-
0.75	3.6445e+000	-	-
0.80	3.6513e+000	-	-
0.85	3.6593e+000	-	-
0.90	3.6693e+000	-	-
0.91	3.6718e+000	-	-
0.92	3.6744e+000	-	-
0.93	3.6773e+000	-	-
0.94	3.6806e+000	-	-
0.95	3.6843e+000	-	-
0.96	3.6887e+000	-	-
0.97	3.6940e+000	-	-
0.98	3.7012e+000	-	-
0.99	3.7125e+000	-	-

Dose	Tries	Hits
1.0443e+000	1	0
1.2143e+000	1	0
1.7243e+000	1	0
1.7728e+000	1	0
2.0157e+000	1	0
2.3678e+000	1	0
3.0357e+000	1	0
3.3999e+000	1	0
3.8492e+000	1	1
4.7235e+000	1	1
5.8285e+000	1	1
9.1070e+000	1	1
	12	4

**********Original Data**********

1.04427	0	1.21426	0	1.72426	0	1.77283	0
2.01568	0	2.36782	0	3.03566	0	3.39994	0
3.84922	1	4.72349	1	5.82847	1	9.10699	1

Appendix B

O-5: Output of Probit calculation for measurements of frozen pig eyes at 2.7 μm

ONES = 10 ZEROES = 4
h = 0.00
g = 0.000
t = 1.960
Percent confidence = 0.95
SYY = 0.000
SXY = 0.000
SXX = 0.000
S0 = 0.000
ED50 = 8.8417e-001
FLU = 8.8417e-001
FLL = 8.8417e-001
Pearson's Chi-Sq = 0.0000 Probability of Chi-Sq = 1.0000
Log XBAR = -0.0544
Log YBAR = 4.8121
Intercept = 10.7306
Slope = 200.7110
Iterations = 38

Prob	Dose	Lower Limit	Upper Limit
0.01	8.6089e-001	- -	
0.02	8.6358e-001	- -	
0.03	8.6530e-001	- -	
0.04	8.6659e-001	- -	
0.05	8.6765e-001	- -	
0.06	8.6854e-001	- -	
0.07	8.6933e-001	- -	
0.08	8.7004e-001	- -	
0.09	8.7068e-001	- -	
0.10	8.7127e-001	- -	
0.15	8.7372e-001	-	-
0.20	8.7568e-001	-	-
0.25	8.7736e-001	-	-
0.30	8.7887e-001	-	-
0.35	8.8027e-001	-	-
0.40	8.8161e-001	-	-
0.45	8.8290e-001	-	-
0.50	8.8417e-001	-	-
0.55	8.8545e-001	-	-
0.60	8.8675e-001	-	-
0.65	8.8809e-001	-	-

0.70	8.8951e-001	-	-
0.75	8.9104e-001	-	-
0.80	8.9275e-001	-	-
0.85	8.9475e-001	-	-
0.90	8.9727e-001	-	-
0.91	8.9788e-001	-	-
0.92	8.9854e-001	-	-
0.93	8.9927e-001	-	-
0.94	9.0009e-001	-	-
0.95	9.0102e-001	-	-
0.96	9.0211e-001	-	-
0.97	9.0346e-001	-	-
0.98	9.0525e-001	-	-
0.99	9.0809e-001	-	-

Dose	Tries	Hits
4.0379e-001	1	0
6.1376e-001	1	0
6.4606e-001	1	0
8.0758e-001	1	0
9.6910e-001	2	2
1.2114e+000	1	1
1.4536e+000	1	1
2.2612e+000	2	2
2.8265e+000	2	2
4.6840e+000	1	1
4.7647e+000	1	1
	14	10

**********Original Data**********

0.40379	0	0.61376	0	0.64606	0	0.80758	0
0.9691	1	0.9691	1	1.21137	1	1.45364	1
2.26123	1	2.26123	1	2.82653	1	2.82653	1
4.68397	1	4.76472	1				

Appendix B

O-6: Output of Probit calculation for measurements of frozen pig eyes at 2.5 μm

ONES = 4 ZEROES = 5
h = 0.00
g = 0.000
t = 1.960
Percent confidence = 0.95
SYY = 0.000
SXY = 0.000
SXX = 0.000
S0 = 0.000
ED50 = 3.6794e+000
FLU = 3.6794e+000
FLL = 3.6794e+000
Pearson's Chi-Sq = 0.0000 Probability of Chi-Sq = 1.0000
Log XBAR = 0.5682
Log YBAR = 5.4122
Intercept = -94.3152
Slope = 166.7019
Iterations = 41

Prob	Dose	Lower Limit	Upper Limit
0.01	3.5630e+000	- -	
0.02	3.5764e+000	- -	
0.03	3.5850e+000	- -	
0.04	3.5914e+000	- -	
0.05	3.5967e+000	- -	
0.06	3.6012e+000	- -	
0.07	3.6051e+000	- -	
0.08	3.6086e+000	- -	
0.09	3.6118e+000	- -	
0.10	3.6148e+000	- -	
0.15	3.6271e+000	-	-
0.20	3.6368e+000	-	-
0.25	3.6452e+000	-	-
0.30	3.6528e+000	-	-
0.35	3.6598e+000	-	-
0.40	3.6665e+000	-	-
0.45	3.6730e+000	-	-
0.50	3.6794e+000	-	-
0.55	3.6857e+000	-	-
0.60	3.6923e+000	-	-
0.65	3.6990e+000	-	-

0.70	3.7061e+000	-	-
0.75	3.7138e+000	-	-
0.80	3.7224e+000	-	-
0.85	3.7324e+000	-	-
0.90	3.7451e+000	-	-
0.91	3.7481e+000	-	-
0.92	3.7515e+000	-	-
0.93	3.7551e+000	-	-
0.94	3.7592e+000	-	-
0.95	3.7639e+000	-	-
0.96	3.7694e+000	-	-
0.97	3.7762e+000	-	-
0.98	3.7852e+000	-	-
0.99	3.7995e+000	-	-

Dose	Tries	Hits
1.5178e+000	1	0
1.7607e+000	1	0
2.0642e+000	1	0
2.6714e+000	1	0
3.2785e+000	1	0
4.1285e+000	1	1
4.3713e+000	1	1
5.3428e+000	1	1
7.5284e+000	1	1
	9	4

**********Original Data**********

1.51783	0	1.76068	0	2.06425	0	2.67138	0
3.27852	0	4.1285	1	4.37135	1	5.34277	1
7.52844	1						